DOKUZ EYLÜL UNIVERSITY

GRADUATE SCHOOL OF NATURAL AND APPLIED SCIENCES

NUMERICAL INVESTIGATION OF CONDENSATION ON HORIZONTAL FLAT PLATE

by

S. Sedin GÜRBÜZ

September, 2013

İZMİR

NUMERICAL INVESTIGATION OF CONDENSATION ON HORIZONTAL FLAT PLATE

A Thesis Submitted to the
Graduate School of Natural and Applied Sciences of
Dokuz Eylül University
In Partial Fulfillment of the Requirements for the Degree of Master of Science
in Mechanical Engineering, Thermodynamics Program

by
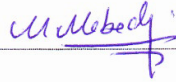**S. Sedin GÜRBÜZ**

September, 2013
İZMİR

M.Sc. THESIS EXAMINATION RESULT FORM

We have read the thesis entitled **"NUMERICAL INVESTIGATION OF CONDENSATION ON HORIZONTAL FLAT PLATE"** completed by **S.SEDİN GÜRBÜZ** under supervision of **ASSOC. PROF. DR. AYTUNÇ EREK** and we certify that in our opinion it is fully adequate, in scope and quality, as a thesis for the degree of Master of Science.

Assoc. Prof. Dr. Aytunç EREK

Supervisor

Doç. Dr. Moghtada MOBEDi

(Jury Member)

Yar. Doç. Dr. Can Özgür Golpan

(Jury Member)

Prof. Dr. Ayşe OKUR

Director

Graduate School of Natural and Applied Sciences

ii

ACKNOWLEDMENTS

I would like to thank to my supervisor, Assoc. Prof. Dr. Aytunç EREK, for his unlimited support and guidance during the study and his contribution to the achievements of this work is significant.

I would also like to thank to my friend, Assist. Mehmet Akif EZAN, for his help and support. Special thanks to my family and all my friends.

<div align="right">S. Sedin GÜRBÜZ</div>

NUMERICAL INVESTIGATION OF CONDENSATION ON HORIZONTAL FLAT PLATE

ABSTRACT

In this study, condensation of humid air is examined on a horizontal flat plate numerically. When the humid air flows on the cold surfaces, it begins condensation and then solidification on the surface. The condensation on surface reduces the heat transfer rate and increases pressure drop.

Geometry of horizontal flat plate is generated in GAMBIT software. The geometry is divided into small parts with suitable mesh sizes. Initial and boundary conditions are used to solve governing equations which are continuity, momentum, energy and species equations. Using FLUENT software, temperature distribution, velocity distribution, condensation mass flux rate and net heat transfer rate are observed. A comparison between numerical results and analytical results are performed for condensation mass flux on flat plate. To solve condensation on flat plate User Defined Function code is used in FLUENT which is prepared with C++ software. Then condensation is calculated numerically which is from humid air to the flat plate. For the higher inlet velocity values, heat transfer rate increases. For the higher inlet temperature, the higher heat is transferred but lower mass flux is observed. For the lower mass fraction, the lower net heat transfer is observed.

Keywords: Condensation, humid air, numerical modeling, UDF.

YATAY DURAN DÜZ LEVHA ÜZERİNDEKİ YOĞUŞMANIN SAYISAL OLARAK İNCELENMESİ

ÖZ

Bu çalışmada, yatay düz levha üzerindeki yoğuşma nümerik olarak incelenmiştir. Nemli hava soğuk bir yüzey üzerinden akarken önce yoğuşmaya başlar ve daha sonra yüzey üzerinde katılaşır. Yüzey üzerindeki yoğuşma ısı transferini azaltır ve basınç düşümünü arttırır.

Yatay düz levha geometrisi GAMBIT programında oluşturulmuştur. Uygun mesh kalitesi kullanılarak küçük hacimlere bölünmüştür. Süreklilik, momentum, enerji ve tür denklemlerini çözmek için sınır ve başlangıç koşulları kullanılmıştır. FLUENT programını kullanarak, sıcaklık dağılımı, hız dağılımı, yoğuşan kütle akısı ve net ısı transferi değerleri gözlenmiştir. Yatay düz levha üzerindeki yoğuşan kütle akısı nümerik ve analitik sonuçlarla karşılaştırılmıştır. FLUENT' de yoğuşmayı çözmek için C++ programında oluşturulmuş User Defined Function kodu kullanılmıştır. Daha sonra nemli havadan düz yüzey üzerine olan yoğuşma miktarı hesaplanmıştır. Daha yüksek giriş hızı olması, daha yüksek ısı transferi olmasına sebep olmuştur. Daha yüksek giriş sıcaklığı olması, daha yüksek ısı transferi olmasını sağlamış fakat daha düşük kütlesel akı gözlenmiştir. Daha düşük kütle kesri daha düşük net ısı transferine sebep olmuştur.

Anahtar Kelimeler: Yoğuşma, nemli hava, sayısal modelleme, UDF.

CONTENTS

LIST OF FIGURES

Page

LIST OF TABLES

CHAPTER ONE
INTRODUCTION

Condensation in heat exchangers has become so important recently. A heat exchanger generates to ensure that heat transfer occurs efficiently. But the heat transfer is decreased by condensation on fins. The heat exchanger is separated by solid walls which are called fins. So that fluid can flow between them. Heat exchangers are commonly utilized in refrigeration, petroleum refineries, power plants, air conditioning, petrochemical plants and chemical plants. The similar of heat exchanger is found in a refrigeration that (circulating fluid is known refrigerant fluid) flows through tubes. Air flows between fins which cools the incoming air.

Condensation is formed with humid air flow in heat exchanger. Humid air flows between cold fins in heat exchanger. The fins are cold because of refrigerant fluid so the frost formation will be formed. The heat transfer on the surface decreases cause of frost. Also frost increases the pressure drop. If heat exchanger will be designed, the frost effects must be known exactly.

The frost formation on flat plate is examined by Yonko & Sepsy (1967) and heat transfer of frost is declared. Also frost formation is examined by Jones & Parker (1975) on flat plate. Also frost formation rate is increased cause of relative humidity. If the inlet velocity is increased, frost formation decreases. Hayashi, Aoki, Adachi & Hori (1977) described the frost formation in three scenes. In those scenes, The frost becomes one dimensional and then frost is become three-dimensional. The frost on flat plate is been spongy. The frost density on cold plate is computed and then the frost thickness of model is computed on cold plates by Sami & Duong (1989). Conclusions showed that if surface temperature decreases or relative humidity increases, frost formation is increasing. Tao, Besant & Mao (1993) are studied for frost formation which is formed with forced convection conditions on cold plate. Gradual continuous model is examined by Sherif, Raju, Padki & Chan (1993).
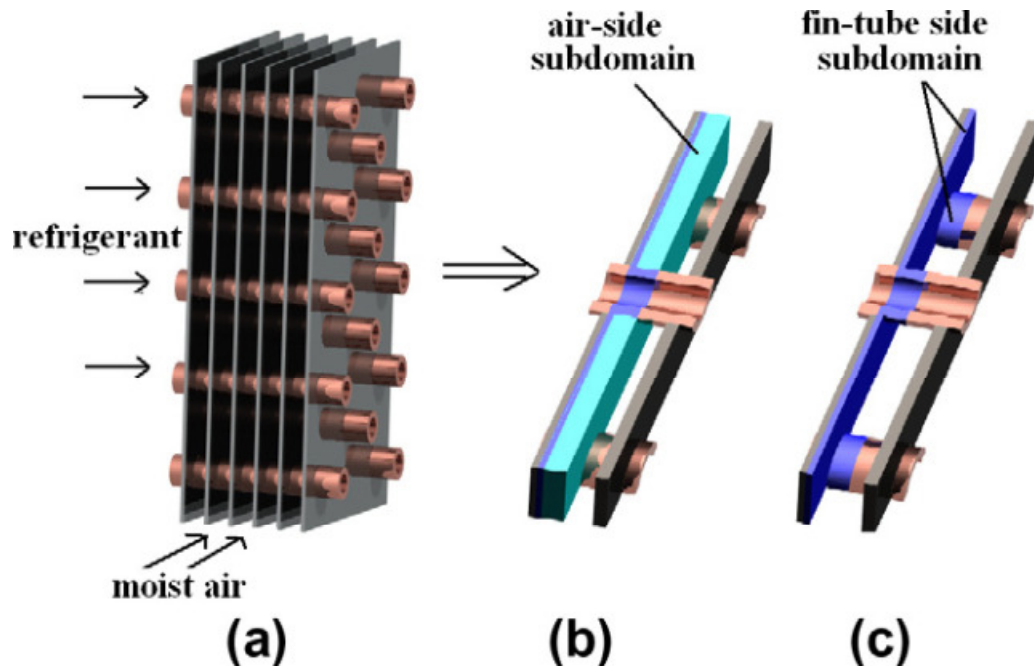
Figure 1.1 View air-side and fin-tube side of heat exchanger (Cui, J., Li, W. Z., Liu, Y., & Zhao, Y.S. 2011)

Heat exchangers are used in many sectors commonly, especially fin and tube heat exchangers. So they are examined by many studies cause of importance. Shepherd (1956), Saboya & Sparrow (1974), Saboya & Sparrow, (1976) and Kuan, Aris, Rosman & Davis (1984) studied on heat exchangers which are containing circular tubes and plate fins. The most common information is existing in the literature by them. Different heat exchanger configurations are investigated.

Shepherd (1956) formed leader article of regulations with one row of circular tubes. The fins are assumed isothermal. So heat transfer coefficients are defined as a function of the Reynolds. Forced convection and the effect of condensation are examined for laminar boundary layer flow by Sparrow & Saddy (1967) analytically. The analysis is realized with noncondensable gas and vapor, so exact comprehensive conclusions are found. Integral method is used to obtain conclusions of the similarity differential equations, numerically. Different boundary conditions are used to solve problem. So heat transfer from moist air is compared easily. If the pressure value is

2

low, the heat transfer decreases. So decrease of heat transfer is emphasized in the article. The other important subject is gravity in forced flow. It is more precision than condensation. Also interface temperature is investigated. The temperature values change at the interface. The results are displayed an insignificant effect on the heat transfer. Saboya & Sparrow (1974) are investigated the naphthalene sublimation technique.

Global heat and mass transfer coefficients are found experimentally for different heat exchanger types. Three-row heat exchangers are expanded by Saboya & Sparrow (1976). Behind the tubes are obtained low mass transfer coefficients from the results. Rosman et al (1984) studied experimentally and numerically. Different heat exchanger types is examined for heat transfer coefficients and mass transfers. Then temperature distribution of fins are examined. So fin efficiency is found. Liang, Wong & Nathan (2000) studied for fin efficiency of heat exchangers which have moist air flow. Suitable solution is found with comparing one dimension and two dimension models, analytically and numerically. One dimensional model is solved numerically. The local mass transfer effect is considered for this model. The fins geometry is so different for two dimensional model. McQuiston's methods are used for comparison of these models method.

Kakac & Liu (2002) investigated to design of the heat exchangers. Fossa & Tanda (2002) studied for importance of frost formation in refrigeration equipment and investigated heat transfer which occurs between vertical plates. Frost formation is investigated experimentally. The glycol cooled plate with the internal circulation. Plate is in a vertical channel. So the natural circulation occurred on vertical plate. Humid air are investigated with 31-85% relative humidity, also 26-28°C temperature. Seker, Karatas & Egrican (2003) studied for frost formation on heat exchanger, numerically. Also the heat and mass transfer characteristics are examined. Humid air-frost layer interface temperature is found. The mass flow rate is computed on the surface. The heat exchanger's surface efficiency also is calculated. Pressure drop is examined in the article. So different inlet parameters are used to solve the problem which are mass flow rate, relative humidity, inlet temperature etc.

3

Yang & Sektar (2007) studied for heat and mass transfer. Humid air problem is solved by using CFD modeling. Single coil twin fan is examined to improve of their cooling capacities. The SCTF system is displayed its capability to ensure improved air feature and success important energy savings in archetype experiments. But, they select with forecast geometric parameters, which performs parametric optimization efforts. CFD simulation is selected to solve problem. Because it has economic importance and flexibility; compartmented coil is so expensive. To compute the latent heat transfer, the recently advanced numerical algorithm is used. This algorithm is formed FLUENT software, professionally. Analytical solution is used to confirm for a basic two-dimensional case. Different parametric optimization is performed for solutions which are confirmed by experimental data.

Laaroussi & Lauriat (2008) studied for enclosures which has two dimension and condensation on surface. Also heat transfer on the surface is computed numerically. Model's wall is performed suitable thickness. Then cold air is existed behind walls. Benelmir, Mokraoui & Souayed (2009) studied for the simulation of humid air flow two vertical plates. So condensation is formed on the surfaces. Then condensation is solved using Fluent software. The finite volume method combined the differential equations which are used for the heat and mass transfer, in two and three dimensions. The mixture boundary layer equations are calculated firstly without considering the condensate thickness. Later for the humid air condensation effect is considered a specific program (UDF) improved by Bell. The Fick's law is performed to examine condensate flow on a condensation surface. So a sub-relaxation coefficient is used to provide stability of the model.

Lenic, Trp & Frankovic (2009) studied for frost formation on the surface of a heat exchanger numerically. Also frost formation is examined experimentally for mass transfer. Frost formation required to model complicated mathematical equations which is occurred from humid air to cold surfaces. The problem is unsteady. Mathematical model is improved for frost formation. Then the governing equations are change because of improving. The finite volume methods are used to solve frost formation. Also the simpler algorithm is used for the velocity–pressure

coupling. Frost formation on fins provide to decrease the heat transfer which is showed from results. The frost thickness for different air humidity, temperatures and velocities are investigated from numerical calculations. The mathematical model, the UDF code and the algorithm are used to solve model which are confirmed experimentally. The frost growth conditions are predicted to understand heat flux. Cui, Li, Liu & Zhao (2011) studied to predict the frost behavior with a new CFD model. The frost formation is studied from initial period.. The heat exchangers are researched for performances numerically in the article. Later empirical formulas are occurred in computer. The results are compared with empirical formulas. The local frost formation is calculated. Different parameters is used to understand the effect of frost. At last, the influence factors are also argued, such as relative humidity, fin space and air flow rate.

Condensation on flat plate is examined in this study. Humid air flows on a horizontal flat plate. So humid air becomes cold and then mass diffusion begins. Firstly, UDF code is prepared to find source terms. Condensation is solved in Fluent software. Analytical solution is examined for comparison. Later, different parameters are used to solve for numeric solutions. The effect of mass flow rate, inlet velocity and inlet temperature are obtained numerically. Then they are compared with analytical solutions.

General equations and general mass source for phase change are given in second section. Numerical solutions and comparisons are displayed in third section. Also analytical solution is given in appendix A.

CHAPTER TWO

CONDENSATION OF HUMID AIR ON SURFACE

Condensation is the form changing from gaseous to the liquid phase, and if it happens diversely, it is called as vaporization. When the transition happens from the gaseous phase into the solid phase, it is called deposition. Condensation in the air occurs molecular size by cooling gaseous volume. Rain and snow parts may be given as an example. Condensation occurs according to the temperature of the surface. If the temperature is decreased, frost is formed on flat plate.

Condensation occurs on the plate before frost formation. Condensation of humid air (or other mixture of water vapor and non-condensable gas) plays an important role in many applications.

- Air conditioning equipment
- Fogging on windows
- Heat exchangers in nuclear power plants

In this study, condensation on a horizontal flat plate is examined. Then numerical solutions are compared with analytical solutions. Humidity on a flat plate configuration is analyzed for different geometrical parameters by using a numerical computation technique. In order to find the mass flux rate on a flat plate, several inlet parameters are investigated. The other important point is the heat transfer while moist air flows on flat plate. The effects of the width of moist air domain, inlet moist air velocity, inlet moist air temperature, and inlet mass fraction on mass flux rate and heat transfer across the heat exchanger are investigated for 8 different cases, numerically. Governing equations must be formed firstly. Mass, energy, momentum and species equations are shown in next parts.

2.1 Conservation Equations for Heat and Mass Transfer

2.1.1 Mass Balance

The general mass balance equation in two-dimensional domain can be written as

$$\frac{\partial}{\partial x}(\rho u) + \frac{\partial}{\partial y}(\rho v) = S_{mass} \tag{2.1}$$

where S_{mass} is the source term for the mass balance equation.

2.1.2 Energy Balance

Energy equation for species transport defined as following form,

$$\frac{\partial}{\partial x}(\rho u h) + \frac{\partial}{\partial y}(\rho v h) = \frac{\partial}{\partial x}\left(k\frac{\partial T}{\partial x} - \sum_{i=1}^{n} h_i J_i\right) + \frac{\partial}{\partial y}\left(k\frac{\partial T}{\partial y} - \sum_{i=1}^{n} h_i J_i\right) + S_{energy}$$

where S_{energy} is the source term for the energy balance equation.

2.1.3 Momentum Balance

The momentum balance equations for x- and y- components can be defined as following,

$$\frac{\partial}{\partial x}(\rho u u) + \frac{\partial}{\partial y}(\rho u v) = -\frac{\partial P}{\partial x} + \frac{\partial \tau_{xx}}{\partial x} + \frac{\partial \tau_{xy}}{\partial x} \tag{2.2}$$

$$\frac{\partial}{\partial x}(\rho v u) + \frac{\partial}{\partial y}(\rho v v) = -\frac{\partial P}{\partial x} + \frac{\partial \tau_{yx}}{\partial x} + \frac{\partial \tau_{yy}}{\partial x} \tag{2.3}$$

where P is the pressure for x and y component in the mixture.

2.1.4 Species Balance

The local mass fraction of each species (w_i) is predicted with the solution of the following convection-diffusion equation for the ith species,

$$\frac{\partial}{\partial x}(\rho u w_i) + \frac{\partial}{\partial y}(\rho v w_i) = -\frac{\partial}{\partial x}(J_{i,x}) - \frac{\partial}{\partial y}(J_{i,y}) + R_i + S_i \qquad (2.4)$$

Mass diffusion term differs for laminar and turbulent flow cases,

Mass Diffusion in Laminar Flow

$$J_{i,x} = -\rho D_{i,m}\frac{\partial w_i}{\partial x} \qquad and \qquad J_{i,y} = -\rho D_{i,m}\frac{\partial w_i}{\partial y} \qquad (2.5)$$

where $D_{i,m}$ is the mass diffusion coefficient for species i in the mixture. (Benelmiir and Makroui, 2009)

Total Heat Transfer On Surface

The heat transfer on the surface can be defined as following,

$$q_{net} = \dot{m}'' * \Delta h \qquad (2.6)$$

$$q = \dot{m}''_{ort} * h_{fg} + \dot{m}'' * \Delta h \qquad (2.7)$$

2.2 Analytical Solution

Analytical solution of condensation on a flat plate is taken from Sparrow et al. (1967). Sparrow proves the impact of condensation. This proof is performed as forced condensation and calculations are computed analytically.

The situation under study is pictured schematically in Fig. 2.1. Inlet parameters, interface parameters and coordinate system is illustrated below.
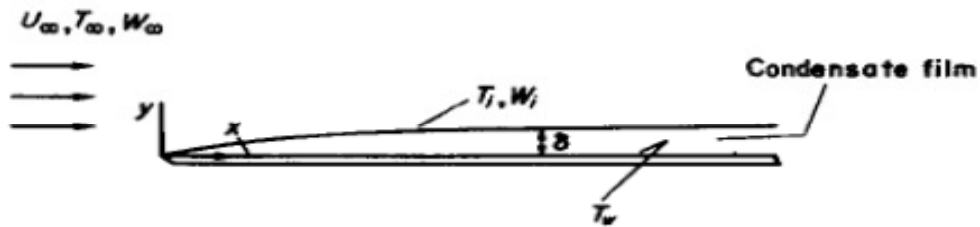
Figure 2.1 Physical model and coordinate system (Sparrow,1967)

Sparrow is examined the flow with two component; vapor and noncondensable gas. w_∞ is showed for inlet mass fraction of noncondensable gas in the flow. T_∞ also is defined inlet temperature. Saturation temperature is computed from partial pressure of the vapor.

This numerical study is compared with analytical solution (Sparrow et al. ,1967). Analytical solution equations are showed in part of appendices clearly. Comparing between numerical and analytical condensation mass flux must be analyzed to show accuracy of the obtained results. So, inlet air mass fraction and wall mass fraction is calculated firstly. The wall temperature is constant (56.85 ^{o}C). Inlet temperature is saturation temperature which has relative humidity in same temperature. The ratio of air mass fraction helps to find η_δ^{-1} and $F(0)$. Then mass flux rate can be drawn along the surface (As given in appendix Eq(8)).

9

2.3 Condensation Model Assumptions

- The vapor phase is consisted of water vapor and air.
- Condensation rate is computed from diffusion in the vapor.
  - This allows the assumption that Ti and Tw, condensation is neglected in the liquid film.
  - Valid under some conditions, but not all. Validity of assumption improves with decreasing condensation rates or increasing air mass fraction.
- No droplet formation in the vapor phase.
- Film wise condensation.
- Velocity is equalized to zero at the interface.
- Condensation is formed from laminar flow.

2.4 Film Condensation Basics

If $T_w < T_{sat}(w_\infty)$ condensation takes place on surface.

- For laminar film flow condensation rate ~ $(T_i-T_w)/d$ where d is the film thickness. (Subscript i : Interface)
- Saturation temperature is reduced and with it the condensation rate.

Liquid – Vapor Interface

Steam + Air Mixture

T_i , w_i

u_∞ , w_∞ , T_∞

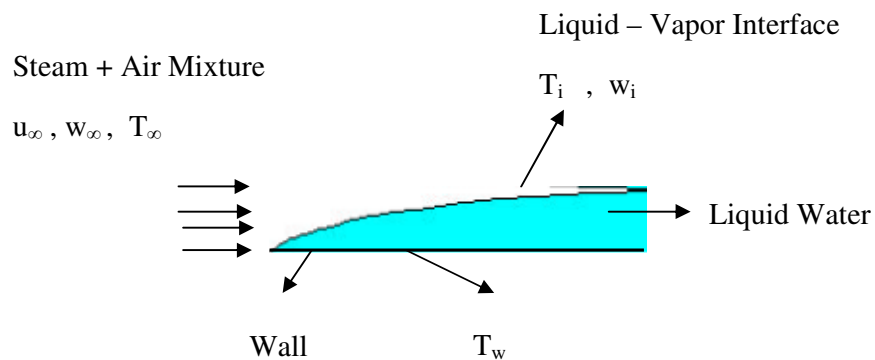Liquid Water

Wall T_w

Figure 2.2 View of film condensation

2.5 Generation of Mass Source for Phase Change

Condensation is examined on cold flat plate. UDF code is prepared to solve condensation. UDF code is developed to computed source terms which are used in the governing equation. UDF code is used in wall adjacent cells. So condensation is computed on the surface. Also species distribution is observed on the surface.
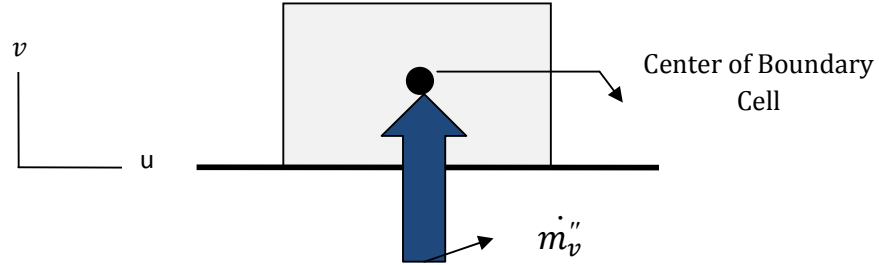
Figure 2.3 Boundary cell of film condensation model

Source terms are implemented in adjacent cells of wall. So, species distribution of condensation and effect of the condensation duration in the humid air is associated into the flow calculations. Species mass fluxes for condensation can be written in first cell on the wall;

$$\dot{m}_a^{''} = \rho_m w_a v - \rho_m D \frac{\partial w_a}{\partial n} \qquad (2.8)$$

$$\dot{m}_v^{''} = \rho_m w_v v - \rho_m D \frac{\partial w_v}{\partial n} \qquad (2.9)$$

Gas mixture's mass fraction is described for binary mixture like (2.10) and (2.11):

$$w_a = 1 - w_v \qquad (2.10)$$

$$\frac{\partial w_a}{\partial n} = - \frac{\partial w_v}{\partial n} \qquad (2.11)$$

11

Add (2.8) and (2.9) and apply (2.10) and (2.11) to get condensation mass flux at:

$$\dot{m}'' = \dot{m}_a'' + \dot{m}_v'' = \rho_m v \qquad (2.12)$$

Only water is situated in the liquid phase,

$$\dot{m}_a'' = 0 \qquad (2.13)$$

Substituting (2.10) and (2.11) into (2.8) and combining with (2.12),

$$\rho_m v = \frac{1}{(w_v - 1)} - \rho_m D \frac{\partial w_v}{\partial n} \qquad (2.14)$$

No-slide boundary condition applies and the interface is a wall boundary in FLUENT, so $\rho_m v$ is equalized to zero in the equation (2.14). Therefore, the condensation rate is specified in the wall adjacent cell.

$$\dot{m}''' = \rho_m v \frac{A_{cellwall}}{V_{cell}} \qquad (2.15)$$

In the UDF, this may be obtained by substituting (2.14) into (2.15). The value of the source term in (2.15) will be negative cause of wall normal vector.

The wall temperature is important in the UDF. Because, saturation temperature of water is considered in UDF. If wall temperature is higher the saturation temperature, humid air mass fraction is adjusted to the worth in the wall adjacent cell.

Amount of mass fraction is not computed at the wall, in FLUENT. Diffusive flux is calculated on surface. So near cell of wall is used to solve on the surface. In order to succeed this, the source term in the species equations must consider to calculate diffusive flux in adjacent cell of wall. Reorganizing (2.15) and substituting with (2.9) and (2.12) into (2.13),

$$\dot{m}''' V_{cell} = \rho_m v w_v A_{cellwall} - \rho_m D \frac{\partial w_v}{\partial n} A_{cellwall} \qquad (2.16)$$

Reorganizing (2.15) and substituting with (2.16),

$$\dot{m}''' V_{cell} = \dot{m}''' w_v V_{cell} - \rho_m D \frac{\partial w_v}{\partial n} A_{cellwall} \qquad (2.17)$$

FLUENT computes the second term on the right hand side of (2.17) is by itself when a constant value is utilized for the boundary condition. Then, in order to provide that FLUENT extracted the amount of water vapor. The amount of water vapor is equal to the condensation in the species equation extracted from the wall-adjacent cell in the continuity equation,

$$\dot{m}''' V_{cell} = \dot{m}_v''' V_{cell} - \rho_m D \frac{\partial w_v}{\partial n} A_{cellwall} \qquad (2.18)$$

Subtracting (2.8) from (2.9) and reorganizing outputs,

$$\dot{m}''' = \frac{\dot{m}_v'''}{w_v} \qquad (2.19)$$

All that leftovers is to represent the volumetric source terms in (2.9).

$$\dot{m}''' = \frac{1}{(w_v - 1)} \rho_m D \frac{\partial w_v}{\partial n} \frac{A_{cellwall}}{V_{cell}} \qquad (2.20)$$

Or, substituting (2.9) into (2.10),

$$\dot{m}_v''' = \frac{w_v}{(w_v - 1)} \rho_m D \frac{\partial w_v}{\partial n} \frac{A_{cellwall}}{V_{cell}} \qquad (2.21)$$

FLUENT software is used to evaluate different parameters. Condensation code is written in the C++ computer language for modeling fluid flow and calculating condensation mass flux rate. Source terms are used in governing equations. So equations (2.21) and (2.19) are used as source code in the UDF.

Source terms for governing equations:

$$S_{mass} = \dot{m}''' = \rho v \frac{A_{cellwall}}{V_{cell}} \qquad (\,2.22\,)$$

$$S_{Species} = \dot{m}''' w_v \qquad (\,2.23\,)$$

$$S_{energy} = \dot{m}''' h_{fg} \qquad (\,2.24\,)$$

2.6 Film Condensation Model

- Liquid-vapor interface is impermeable to air, so condensation mass flux can be written as

$$\dot{m}_v'' = \frac{1}{(w_v - 1)} \; wD \; \frac{\partial w_v}{\partial n} \qquad (\,2.25\,)$$

- Condensation takes part in boundary cells as source term.
    - Mass fraction is adjusted saturation value at wall when temperature < saturation Temperature
    - Source term is function of wall species mass fraction and gradient
    - Utilized with User-Defined Functions.

CHAPTER THREE
CONDENSATION MODEL

3.1 Condensation Model

Humid air is forced to flow over a cold plate in order to calculate condensation mass flux. Then condensation is formed on cold plate clearly. Inlet velocity and water vapor mass fraction values are used to investigate validity of model under different conditions. So, different inlet temperature values and geometrical changes are used to analyze. Width of model is (S) 150 mm and length of model is (L) 1200 mm. Wall temperature is constant at 330K. Density, enthalpy of condensation, thermal diffusion coefficient and specific heat of humid air are taken constant in condensation temperature (T_{wall}).
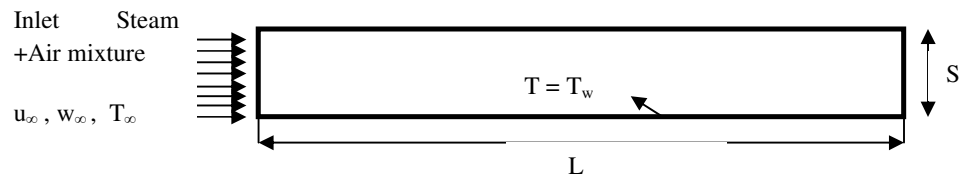

Figure 3.1 View of geometry

3.2 Numerical Analysis

The temperature distribution, velocity distribution and condensation of mass flux over a cold plate surface is determined by FLUENT software. The view of geometry is described in detail in Figure 3.1. UDF code is used to solve this model in FLUENT. The creating and meshing of the model is performed by GAMBIT program. Edges and faces are created and meshed respectively in Figure 3.2. Vertical mesh interval size is 0.001 and ratio is 1.05 from down to up. So mesh interval is increasing down to up. Cause of that 360000 meshes are used to solve problem. Then boundary conditions are used to solve meshed model.
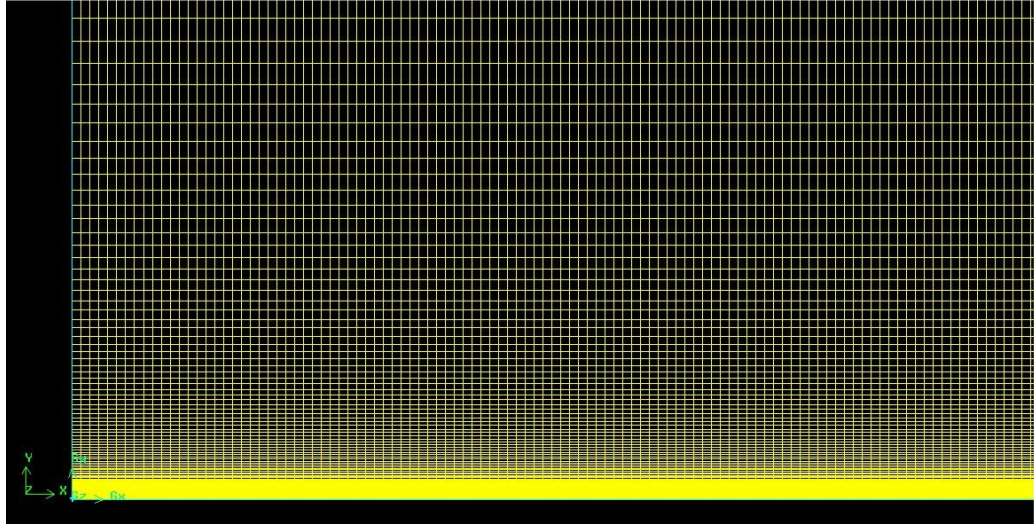
Figure 3.2 Entrance mesh of a part of model

3.3 Boundary Conditions

Two dimensional case is formed to solve condensation model. So, four boundary conditions are used to solve. Velocity inlet boundary condition is defined for left surface, which is illustrated in Figure 3.3. The moist air is exhausted from the right side of the model. So, the outflow boundary condition is given to this surface, in Figure 3.3. Symmetrical boundary condition is applied to the up surface. Plate surface is defined as wall, since convection heat transfer occurs from this surface, shown as down surface in Figure 3.3. Solid and fluid volumes must be defined in order to obtain proper heat transfer results.
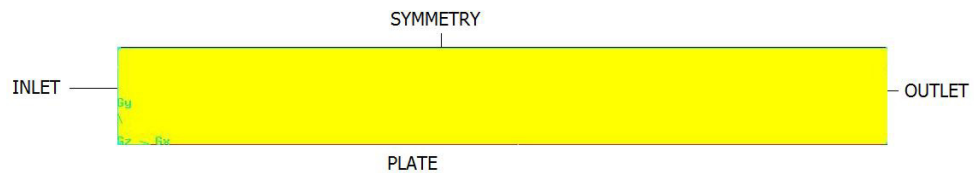

Figure 3.3 Boundary conditions of model

The boundary conditions are given below,

At the inlet:

$$T = T_\infty \quad u = u_\infty \quad w = w_\infty \quad at \quad x = 0 \qquad (3.1)$$

At the plate: (No slide)

$$T = T_w \quad u = 0 \quad w = 0 \quad at \quad y = 0 \; and \quad y = S \; and \; \forall x \quad (3.2)$$

At the symmetry:

$$\frac{\partial T}{\partial y} = 0 \quad u = 0 \quad w = 0 \quad at \quad y = 0 \; and \quad y = S \; and \; \forall x \quad (3.3)$$

In the outlet:

$$\frac{\partial u}{\partial x} = \frac{\partial v}{\partial x} = 0 \quad \frac{\partial T}{\partial x} = 0 \quad at \quad x = L \; and \; \forall y \qquad (3.4)$$

Source terms is used to solve condensation on a surface (Eq. 2.22, Eq. 2.23, Eq. 2,24). So, source terms are added to FLUENT by using UDF code. Therefore source terms are used to solve problem in adjacent cell of the plate (Figure 3.4).
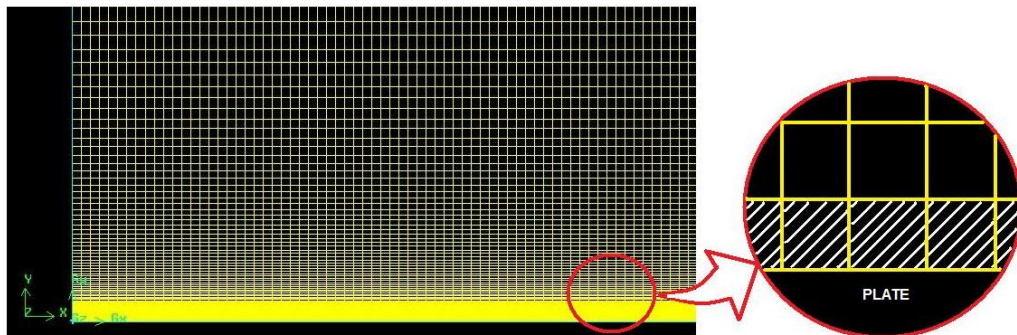

Figure 3.4 Source terms on first cell (Adjacent cell) above plate

CHAPTER FOUR

RESULTS AND COMPARISON WITH ANALYTICAL SOLUTIONS

4.1 Results and Comparison with Analytical Solution

Three different inlet mass fractions and two different inlet velocities are used to compare numerical and analytical solutions. Firstly, inlet temperature is found from saturation temperature. So, analytical results are calculated from dry air mass fraction ratios. To find 'w_w', psychometric diagram is used and calculated in equation (4.1). Wall mass fractions is obtained from condensation value in constant wall temperature. Then $F(0)$ value is calculated for mass fraction equation (As given Table. A.1). Between mass fraction and relative humidity equation is;

$$w = \frac{RH}{1 + RH} \qquad (\ 4.1\ )$$

Inlet velocity, inlet temperature, water vapor mass fraction and wall temperature are varied over range of values to investigate validity of model under different conditions (Table 4.1). Therefore condensation mass flux is calculated easily. Condensation mass flux values are represented same cartesian coordinates (Figure 4.1). Different boundary parameters are illustrated in Table 4.1.

Table 4.1 Boundary parameters

U_∞	w_∞	w_w	$w_{a,\infty} / w_{a,w}$	$F(0)$	T_w	T_∞
0.1 & 1 m/s	0.47967	0.113	0.5866	0.6	330 K	345.64 K
0.1 & 1 m/s	0.33267	0.113	0.7523	0.3	330 K	341.485 K
0.1 & 1 m/s	0.15660	0.113	0.95073	0.05	330 K	336.544 K
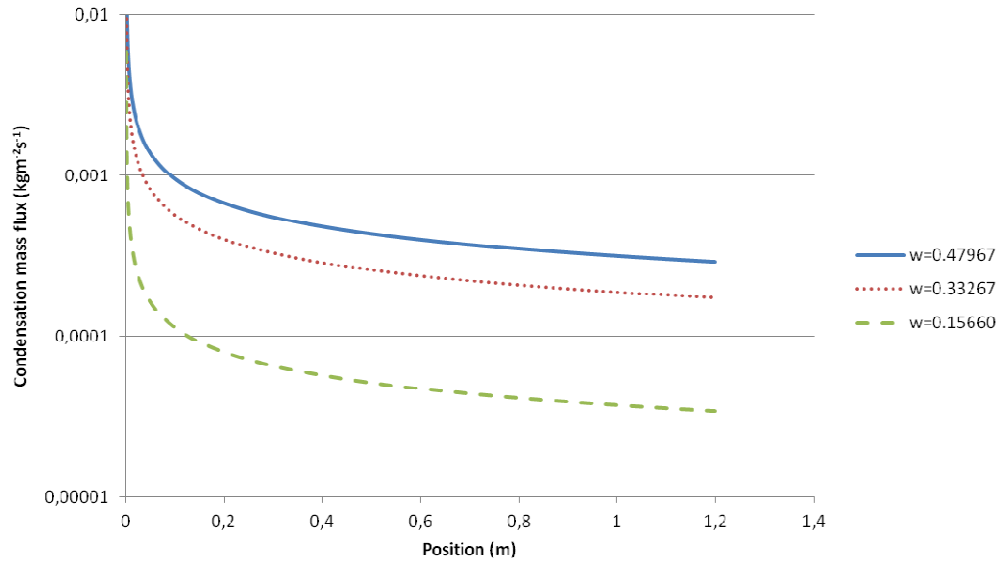
Figure 4.1 Condensation mass flux (u= 0.1 m /s)

Condensation mass flux decreased with reduction of inlet mass fraction (Figure 4.1). Then numerical solutions are compared with analytical solutions. Analytical solutions are calculated from Sparrow et al., (1967), ''Forced Convection Condensation in the Presence of Noncondensables and Interfacial Resistance''. Four CFD solutions with different mass flux values (w_∞) are ;

Figure 4.2 Comparison with analytical solution for air velocity (w_{h2o} =0.15660)

Figure 4.3 Comparison with analytical solution for air velocity (w_{h2o} =0.33267)

Figure 4.4 Comparison with analytical solution for air velocity (w_{h2o} =**0.47967**)
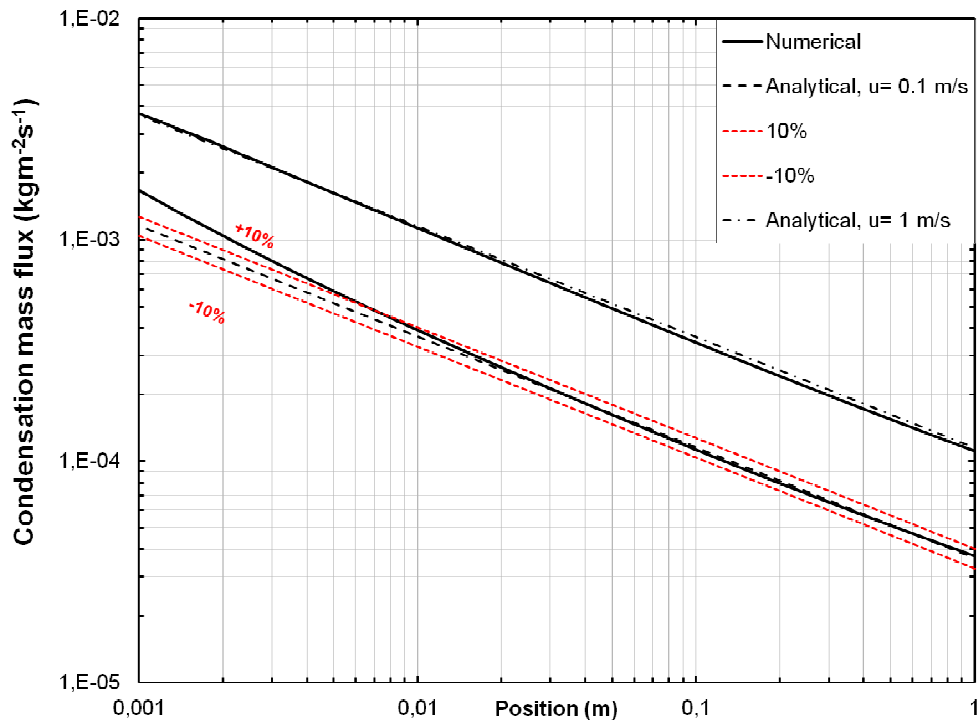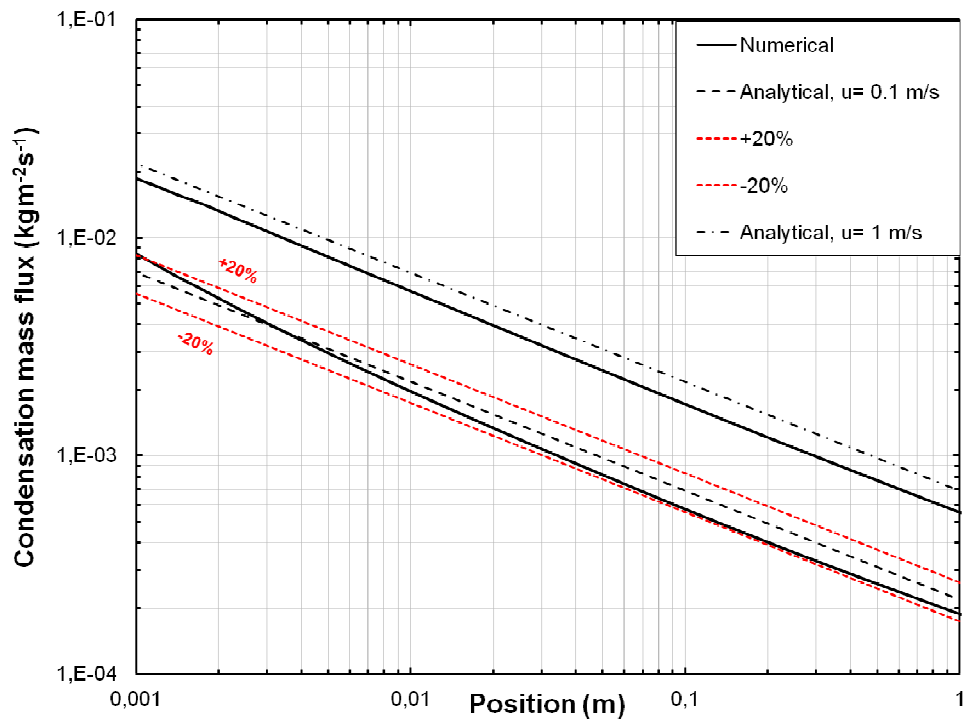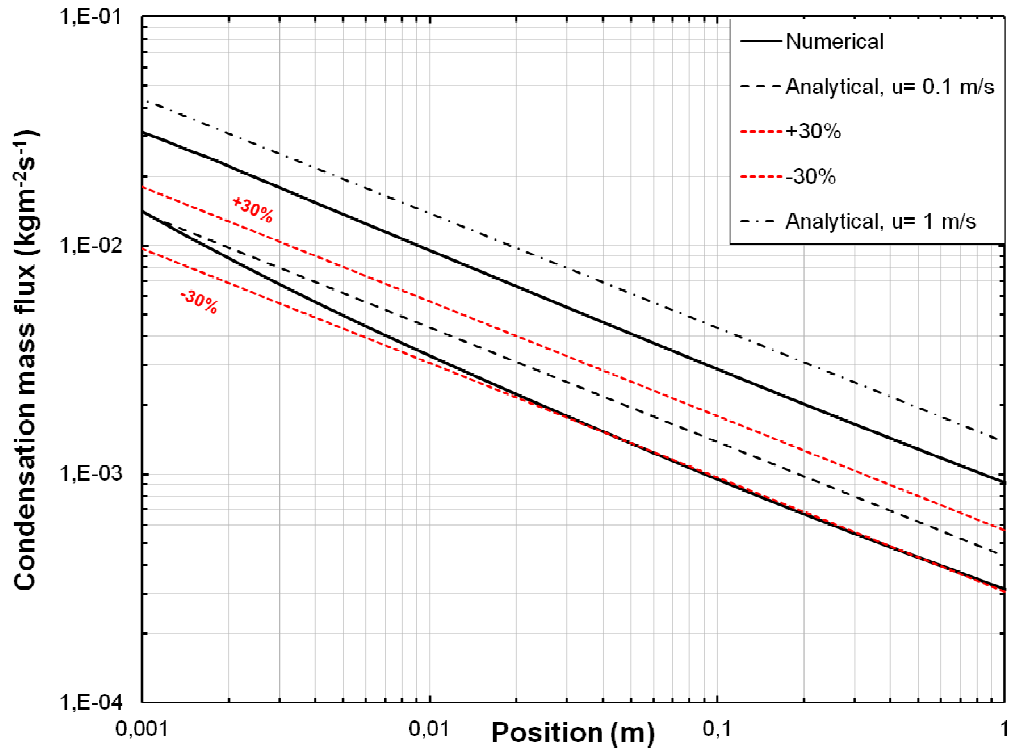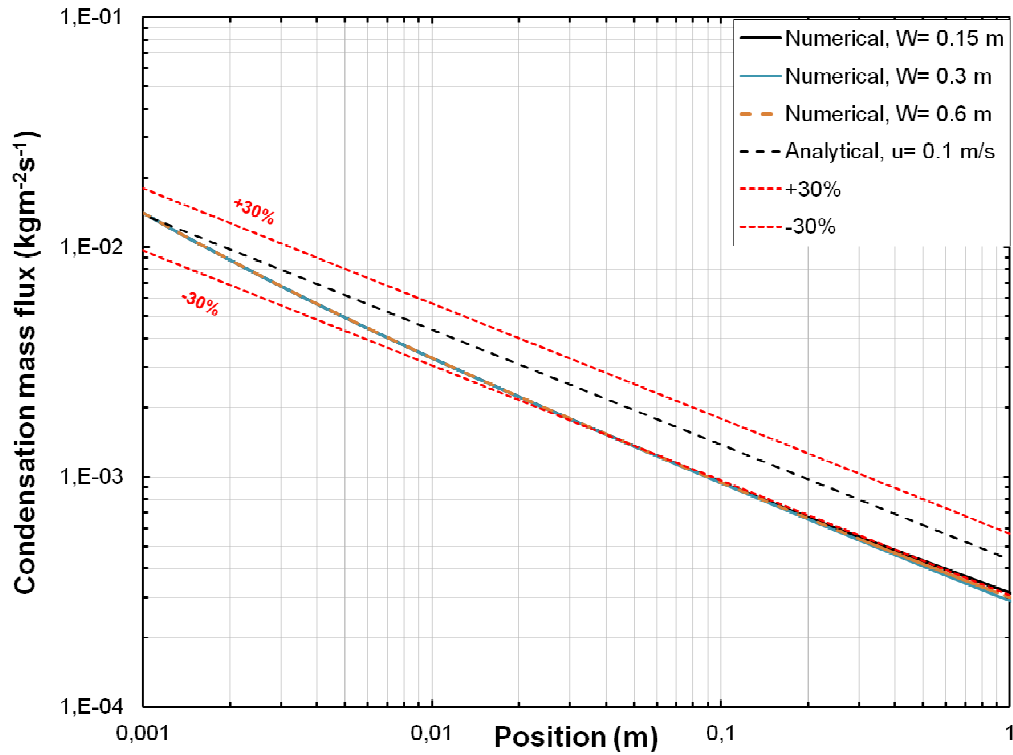

Figure 4.5 Comparison with analytical solution for air velocity (w_{h2o} =**0.47967**)

Differences between CFD results and analytical solutions are showed with errors (Fig. 4.2 to 4.5). The error increases with inlet mass fraction increment. Analytical solutions assumptions are not same with our CFD solutions. The reasons of that errors are geometric boundary conditions and mixture properties. Length and width of cold plate, moist air density, thermal conductivity in FLUENT etc. are different than analytical solutions. And also mesh size can be added to it.

4.2 Results and Discussion of Different Parameters

Comparisons are done by using three inlet humid air fractions and two inlet air velocities. Then domain width of model is changed two different values. So, 8 different cases are studied to examine condensation (Table 4.2). Same mesh, UDF code and boundary conditions are used to solve problem. Temperature distribution, velocity distribution and condensation mass flux is calculated from this models.

Table 4.2 Cases with different boundary parameters

Model	U_∞	T_∞	w_∞	Width (S)
Case 1	0.1 m/s	345.640 K	0.47967	0.15 m
Case 2	0.1 m/s	341.485 K	0.33267	0.15 m
Case 3	0.1 m/s	336.544 K	0.15660	0.15 m
Case 4	0.1 m/s	345.640 K	0.47967	0.30 m
Case 5	0.1 m/s	345.640 K	0.47967	0.60 m
Case 6	1 m/s	345.640 K	0.47967	0.15 m
Case 7	1 m/s	341.485 K	0.33267	0.15 m
Case 8	1 m/s	336.544 K	0.15660	0.15 m

4.2.1 Velocity Distributions
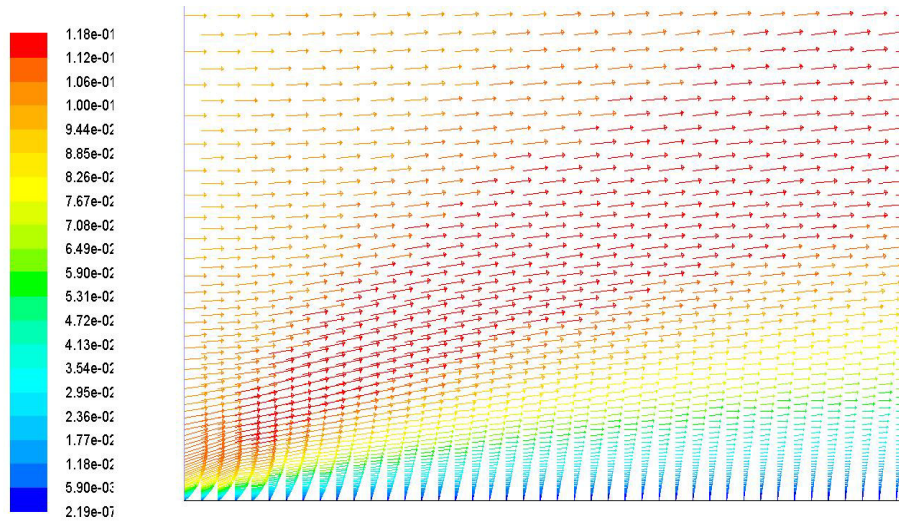
Figure 4.6 A part of velocity distribution on plate of case 1 (m/s)
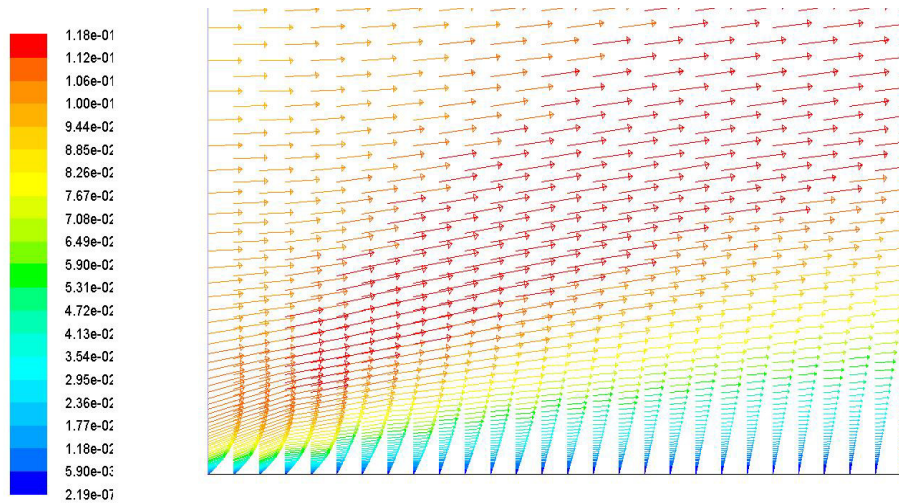
Figure 4.7 A part of velocity distribution on plate of case 2 (m/s)

The effects of the models on velocity vectors and temperature contours are shown in Figure 4.6 to 4.9, respectively. Velocity vector distribution is appeared regularly on cold plate. So, humid air flow is developed regularly along the plate. Velocity is decreasing near plate as expecting.

4.2.2 Temperature Distributions

Figure 4.8 Contour of temperature distribution on plate of case 1 (K)
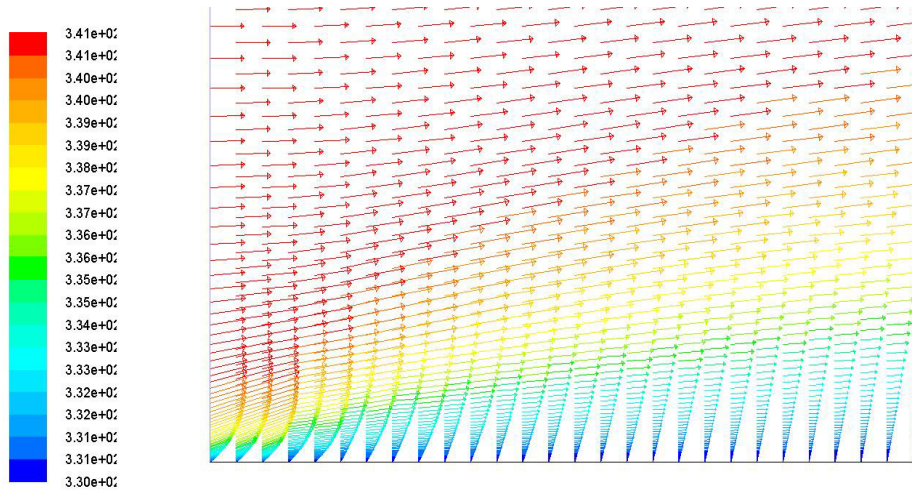
Figure 4.9 A part of vectors of temperature distribution on plate of case 2 (K)

Contours of temperature distribution on plate is given in Figure 4.8. Temperature distribution boundary layer is shown clearly. Temperature is decreasing near plate as expecting, so condensation is expected to form also. Vectors of temperature distribution is appeared regularly in Figure 4.9. So no need to show other cases cause of similarity.

4.2.3 Case 1 (Domain width 0.15 m , Mass Fraction 0.47967)
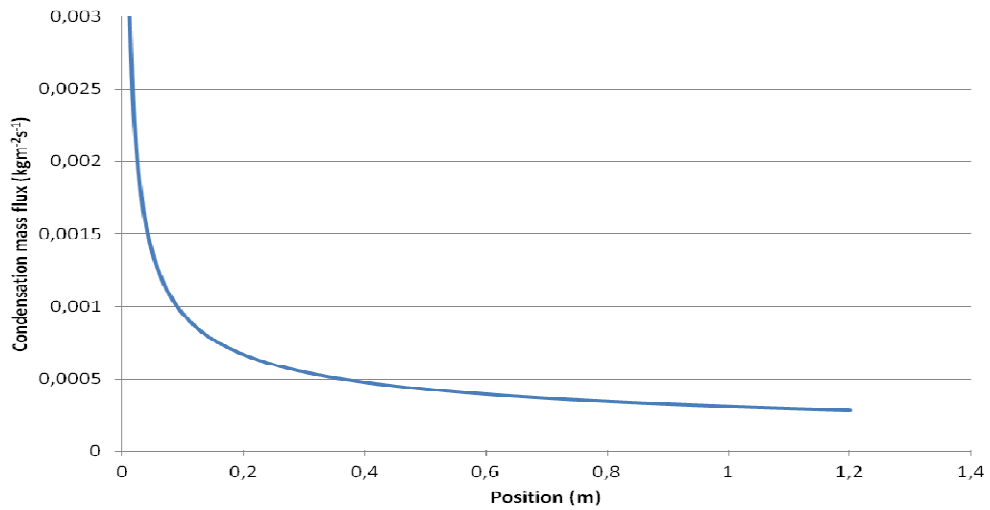
Figure 4.10 Condensation mass flux of case 1

Only condensation mass flux is shown in Figure 4.10 to 4.12. Condensation mass flux values are in case (1) more than the case (2). Also, different mass fraction inlet is important for condensation mass flux. If mass fraction increases, condensation mass flux increases on cold plate.

4.2.4 Case 2 (Domain width 0.15 m , Mass Fraction 0.33267)
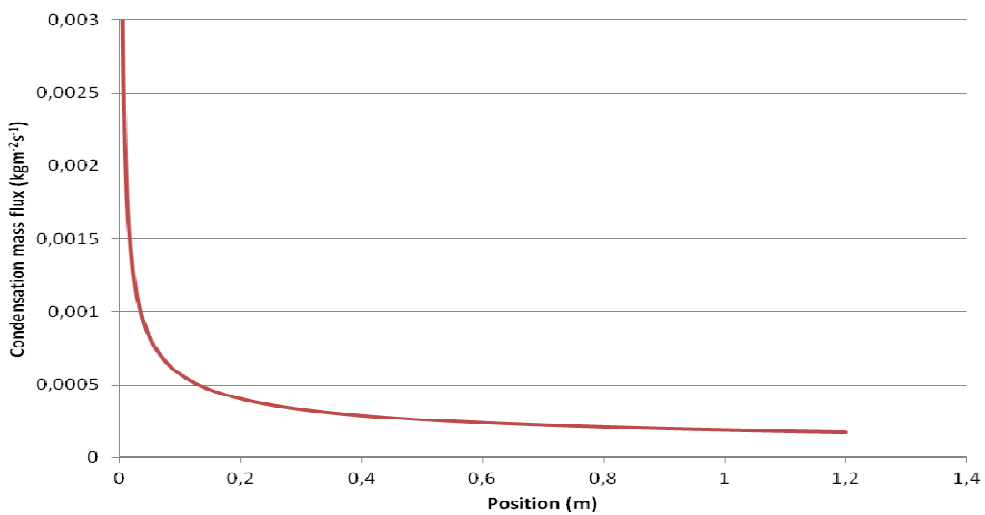
Figure 4.11 Condensation mass flux of case 2

Domain width of case 2 is same with case 1. But mass fraction inlet value is lower than case 1. As a result of this situation condensation mass flux increased. Comparison of condensation mass flux value with case 1 appears clearly in related figures. Condensation mass flux of case 2 is almost same with case 1.

4.2.5 Case 3 (Domain width 0.15 m , Mass Fraction 0.15660)
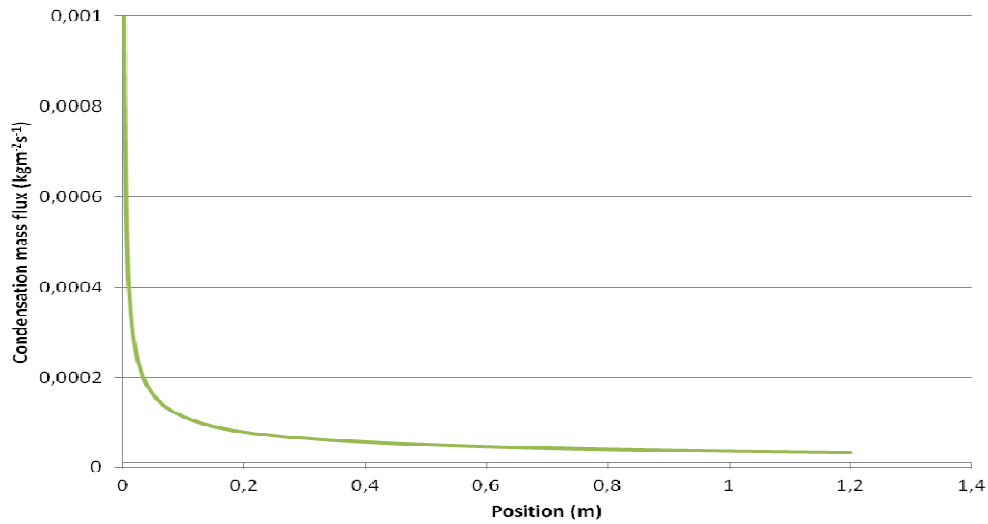
Figure 4.12 Condensation mass flux of case 3

Domain width and velocity inlet are same with case 1. But mass fraction inlet is lowest value of cases. Then condensation mass flux decreases consequently.

Condensation mass flux values of case (1) and case (2) are close, but less mass fraction for case (3) is lower condensation mass flux which is shown in Figure 4.12. Also, condensation mass flux drops three times to lower values.

4.2.6 Case 4 (Domain width 0.3 m , Mass Fraction 0.47967)
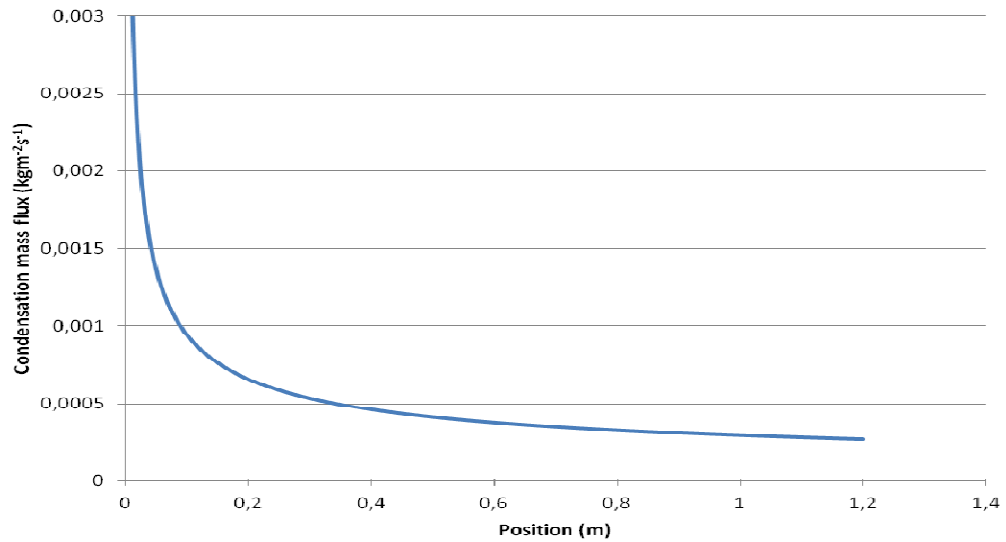
Figure 4.13 Condensation mass flux of case 4

Mass fraction inlet and velocity inlet are same with case 5. But domain width is half of the case 5 value and two times case 1 value. Then condensation mass flux decreases consequently.

4.2.7 Case 5 (Domain width 0.6 m, Mass Fraction 0.47967)
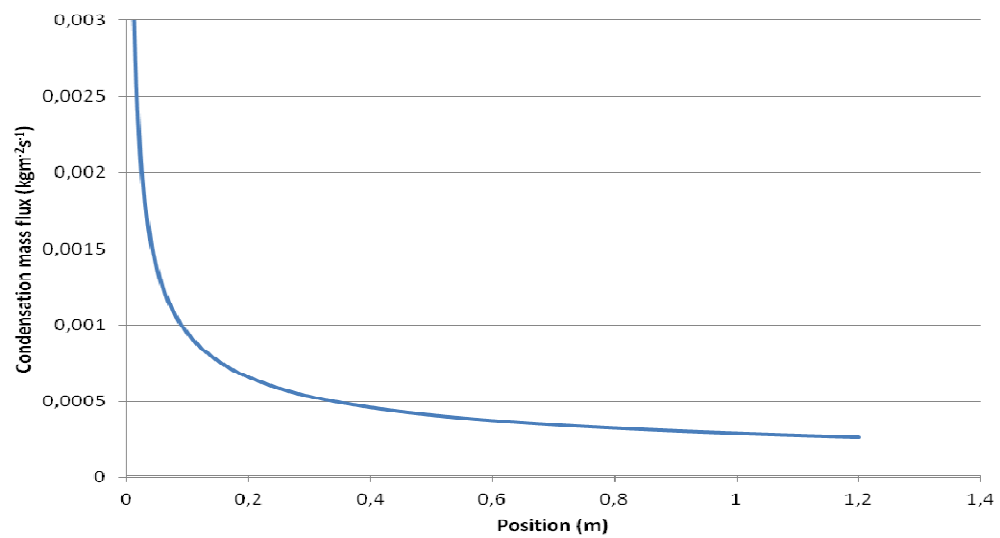
Figure 4.14 Condensation mass flux of case 5

Condensation mass flux values in case (4) and case (5) is so much close, so model domain widths are not influencing mass flux so much. These are shown in Figure 4.13 and Figure 4.14. So heat transfer rate is not changing so much. The effects of width are also showed in comparison between analysis part clearly.

4.2.8 Case 6 (Moist Air Velocity Inlet 1 m/s, Mass Fraction 0.47967)
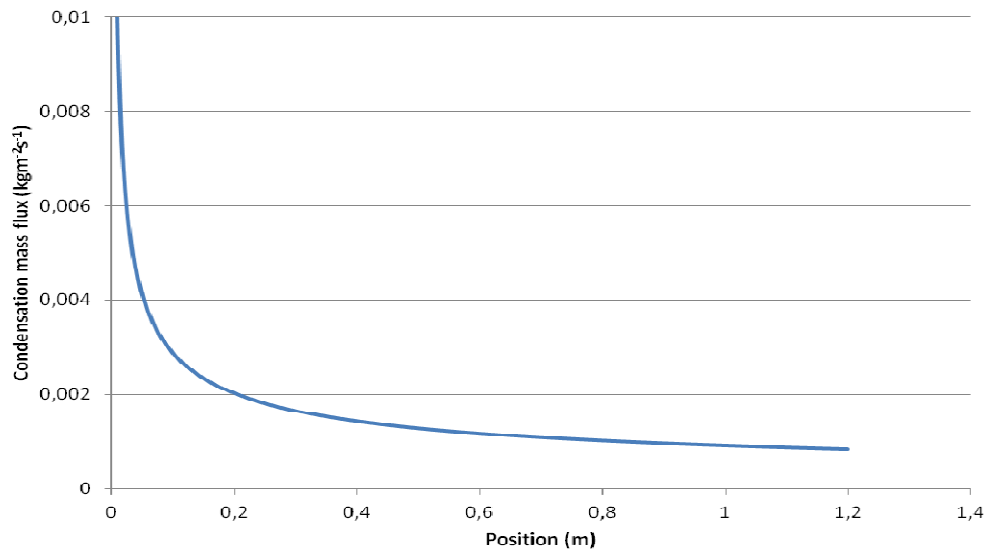
Figure 4.15 Condensation mass flux of case 6

Domain width and velocity inlet of case 6 are same with case 7 and case 8. But mass fraction inlet drops respectively. Then condensation mass flux increases consequently.

4.2.9 Case 7 (Moist Air Velocity Inlet 1 m/s, Mass Fraction 0.33267)
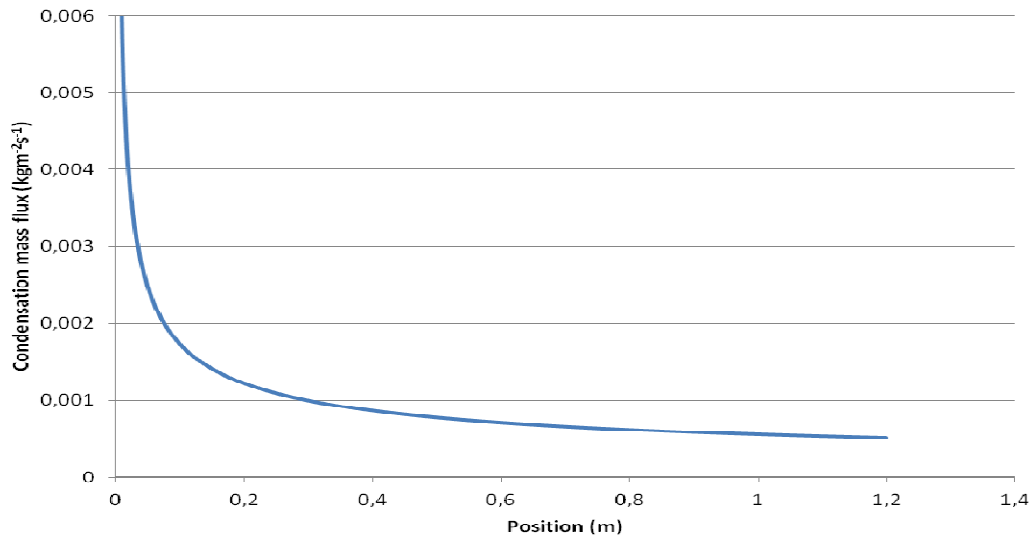
Figure 4.16 Condensation mass flux of case 7

Domain width and velocity inlet of case 7 are same with case 6 and case 8. But mass fraction inlet drops respectively. Then condensation mass flux increases consequently.

4.2.10 Case 8 (Moist Air Velocity Inlet 1 m/s, Mass Fraction 0.15660)
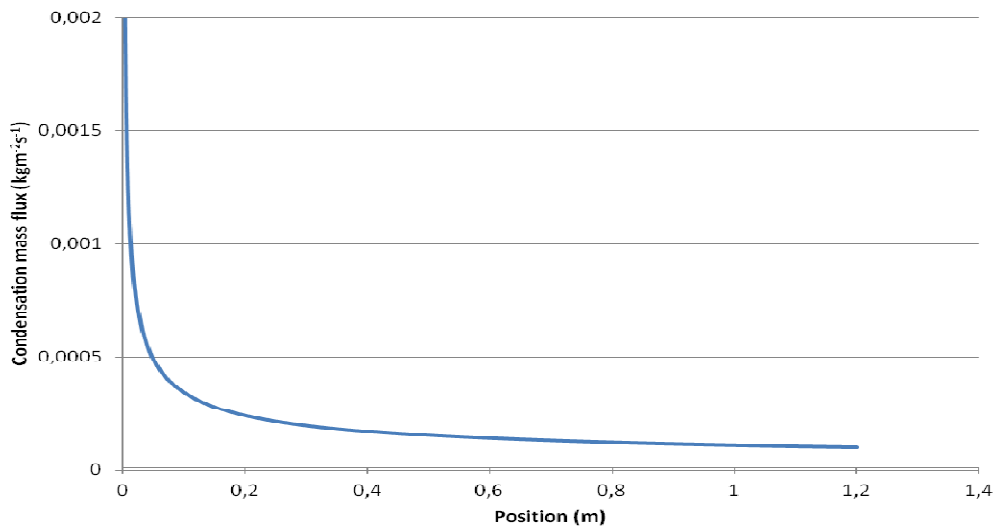
Figure 4.17 Condensation mass flux of case 8

29

Condensation mass flux values in case (6) are highest value of condensation on cold plate (Figure 3.19). Case (7) is showed in Figure 4.16 and case (7) is 0.6 times of case (6). And less mass fraction is case (8) has the lowest condensation mass flux which is shown in Figure 4.17. Also case (8) is about 0.2 times of case (6). So, if inlet mass fraction decreases, condensation mass flux is decreasing.

4.3 Comparison Between Analysis

In this first comparison type, inlet humid air temperature, inlet velocity, inlet mass fraction are T=345.64K , U=0.1 m/s , w = 0.47967. On the flat plate side parameters are T_w = 330 K, w_w = 0.113, L = 1.2 m.
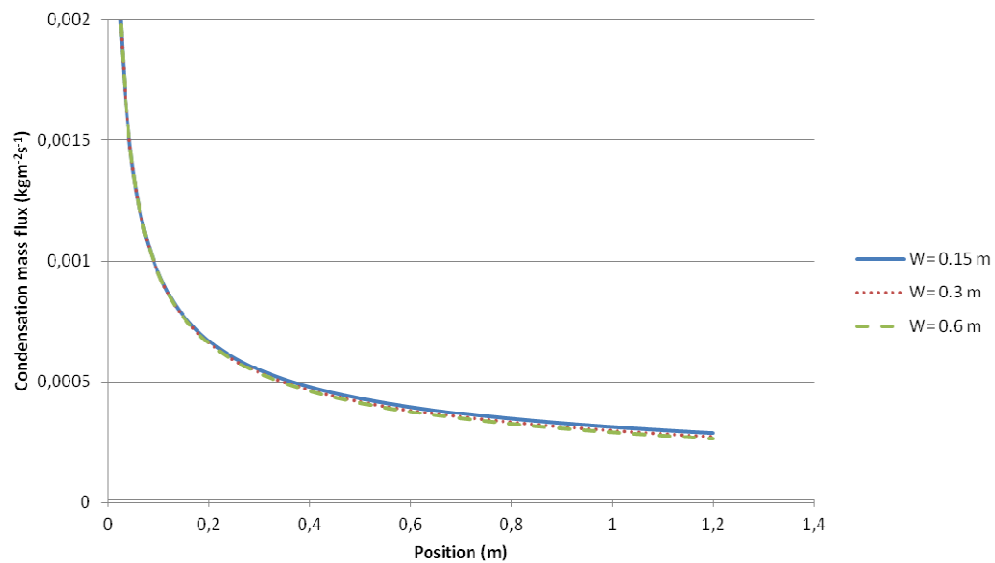
Figure 4.18 Condensation mass flux of 3 different widths

Condensation mass fluxes are shown with comparisons (Figure 4.18 to 4.20). Comparison with different domain widths is in Figure 4.18. Domain width changing is not influence the condensation mass flux so much. So, about same error is calculated in Figure 4.5.

In the second comparison type, inlet velocity is U=1m/s. On the flat plate side parameters are T_w = 330 K, w_w = 0.113, L = 1.2 m, S = 0.15 m.
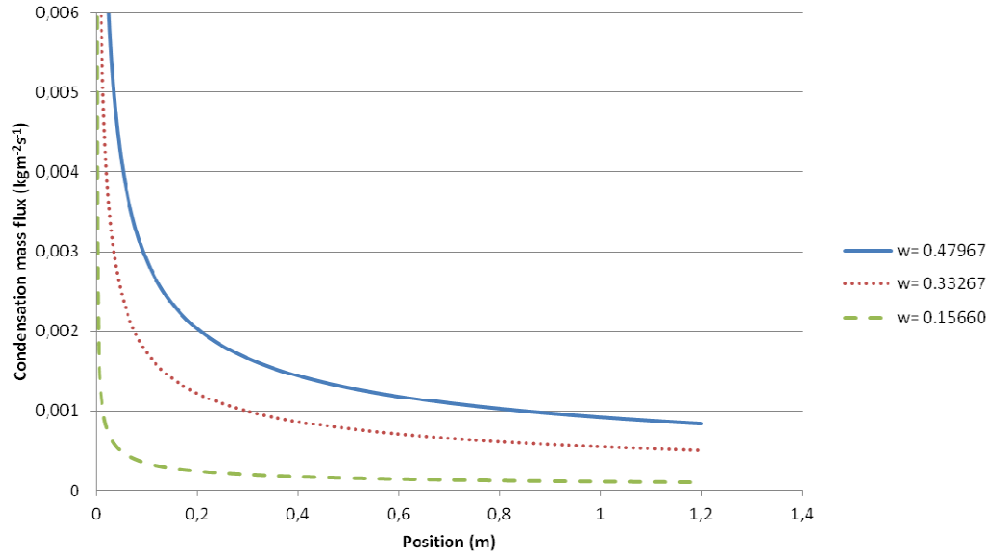
Figure 4.19 Condensation mass flux for U_{in} = 1 m/s

The higher velocity inlet increases mass flux which is shown in Figure 4.19. Velocity inlet is so important for condensation. The highest condensation mass flux is illustrated in Figure 4.19 cause of the highest inlet mass fraction and inlet velocity.

As case (1), case (2) and case (3) (same domain width), the higher mass fraction inlet increases the mass flux which is shown in Figure 4.20. But inlet velocity effect is shown between Figure 4.19 and Figure 4.20 clearly. If the velocity inlet is increased, the condensation mass flux increases about three times on cold plate.

In the third comparison type, inlet velocity is U=0.1 m/s. On the flat plate side parameters are T_{wall} = 330 K, w = 0.113, L = 1.2 m, S = 0.15 m.
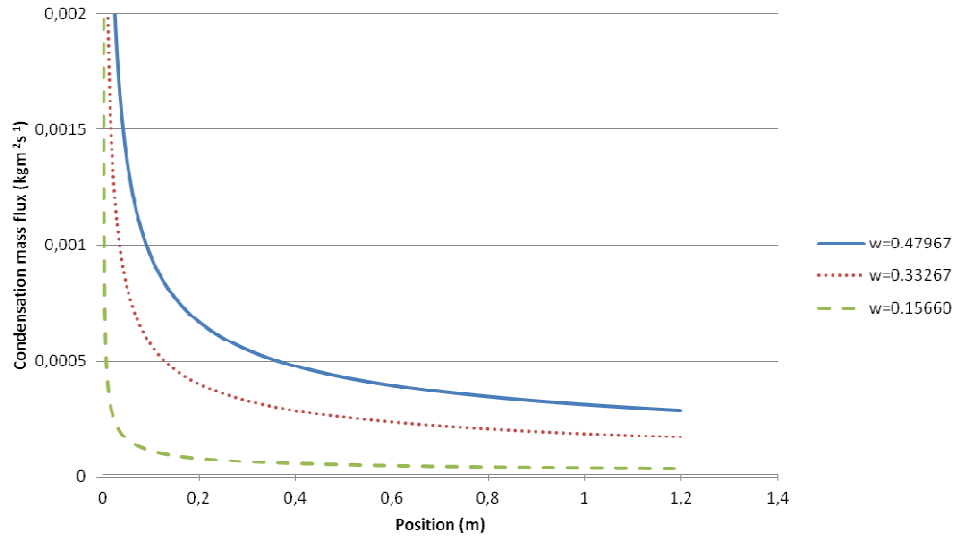
Figure 4.20 Condensation mass flux for $U_{in} = 0.1$ m/s

Inlet temperature (inlet mass fraction) values are changing like that case (6), case (7) and case (8). As case (6), case (7) and case (8) (same domain width and inlet velocity), the higher temperature inlet increases the condensation mass flux which is shown in Figure 4.19. Inlet temperature changing is important for condensation on a cold plate.

Domain width values are changing like that case (1), case (4) and case (5). As case (1), case (4) and case (5) the higher domain width decreases the mass flux which is shown in Figure 4.18. But domain width changing is not important so much. Domain widths of three models are increasing, but condensation mass flux is not changing so much.

4.4 Heat Transfers of Analysis

FLUENT software is run to calculate the heat transfer values for each case. The heat transfer from the humid air which is passing above the cold plate is obtained from the solution of the models, tabulated in Table 4.3 and showed in Figure 4.21.

Table 4.3 Net heat transfer (W)

MODEL TYPE	INLET	OUTLET	NET
Case 1	1124.14 W	-1073.57 W	50.57 W
Case 2	923.80 W	-891.63 W	32.17 W
Case 3	710.21 W	-697.92 W	12.28 W
Case 4	2247.96 W	-2198.61 W	43.35 W
Case 5	4495.59 W	-4446.78 W	48.81 W
Case 6	11238.34 W	-11088.54 W	149.80 W
Case 7	9235.49 W	-9140.36 W	95.13 W
Case 8	7100.49 W	-7064.35 W	36.14 W
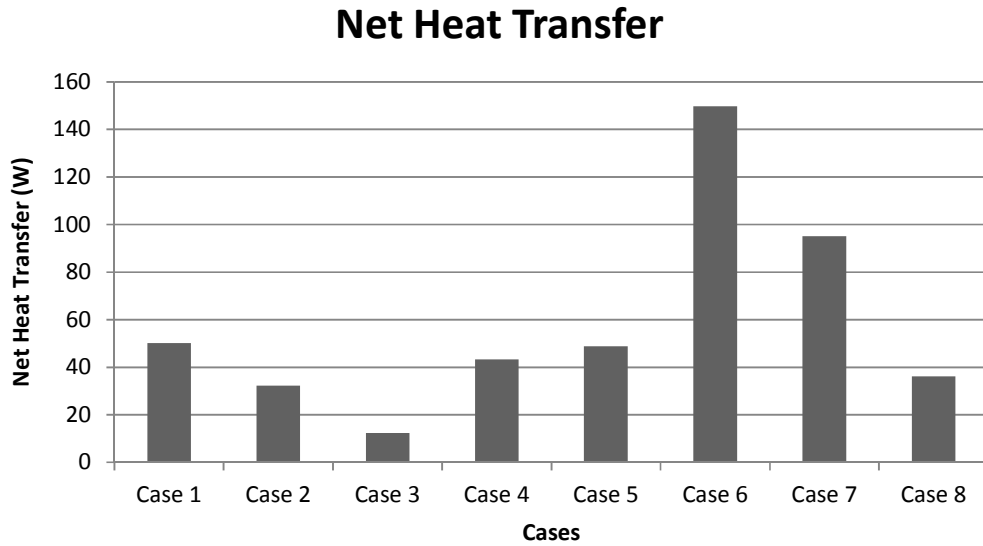
Net Heat Transfer

Figure 4.21 Net heat transfer (W)

In Table 4.3 and Figure 4.21, the effect of the different parameters on the heat transfer rate can be seen in case (6) clearly. The net heat transfer rate is higher than other cases, only for the high inlet velocity and high inlet mass fraction.

Table 4.4 Condensation heat transfer and net heat transfer rate (W)

MODEL TYPE	$\dot{m}''_{ort}$	$\dot{m}''_{ort} * h_{fg}$	NET	TOTAL
Case 1	0,000580	1364.50 W	50.570 W	1415.07 W
Case 2	0,000350	817.460 W	32.170 W	849.630 W
Case 3	0,000069	162.250 W	12.280 W	174.530 W
Case 4	0,000570	1343.89 W	43.350 W	1387.24 W
Case 5	0,000560	1320.31 W	48.810 W	1369.12 W
Case 6	0,001700	3982.19 W	149.80 W	4131.99 W
Case 7	0,001000	2385.70 W	95.130 W	2480.83 W
Case 8	0,000200	477.920 W	36.140 W	514.060 W

Total Heat Transfer
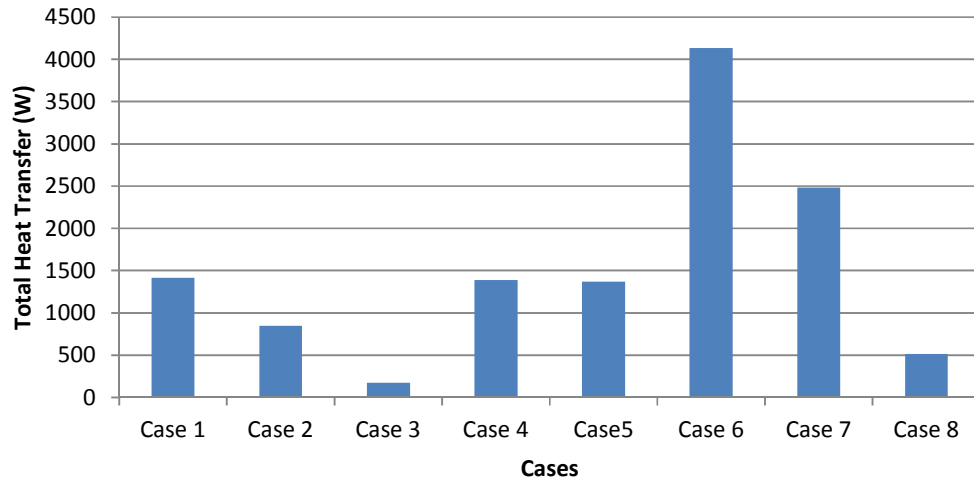
Figure 4.22 Total heat transfer rate (W)

The lower inlet mass fraction has significant effect on net heat transfer rate, as in case (3) has the smallest heat transfer rate (h_{fg}= 2357700 j/kg). When humid air inlet mass fraction is decreased, the lower heat transfer values are obtained, shown in Table 4.4 and Fig 4.22.

CHAPTER FIVE
CONCLUSION

In this study, the condensation mass flux and heat transfer characteristics of horizontal flat plate are performed. Formation of condensation is mentioned firstly. Therefore, analytical solutions are examined to understand how this condensation is solved. Then condensation film basic method is used to solve condensation on cold surface. Humid air is including one phase in domain. Computational Fluid Dynamics (CFD) software, in FLUENT, UDF code is needed to solve this species equations which is written in C++ software. Then a comparison between numerical and analytical results for the mass flux rate and net heat transfer in models are performed.

A comparison between numerical and analytical result for the condensation mass flux ($m_{H_2O}^{''}$) is showed about 10% error. But if the inlet mass fraction increases, the error is increasing. Reasons of error are different properties of humid air, geometrical parameters of model, and mesh counts. The numerical results are reasonably in good agreement with analytical results.

In numerical study, condensation of humid air on cold surface is analyzed for different geometrical and inlet parameters by using FLUENT software. The effects of the domain width, humid air velocity inlet, humid air temperature inlet and humid air mass fraction on condensation mass flux and net heat transfer on cold surface are investigated for 8 different cases. The main conclusions derived from these case studies are:

Higher velocity inlet increases condensation mass flux. If inlet velocity increases, mass flux and heat transfer increases. Case (6) has the highest net heat transfer rate value.

As case (1), case (4) and case (5) the higher domain width decreases the condensation mass flux. But domain width changing is not important so much.

35

Domain widths of three models are increasing, but condensation mass flux is not changing so much.

Greater heat transfer values are obtained as the inlet velocity is increased, as in case (1) and case (6).

If the inlet temperature is increased, heat transfer and condensation mass flux is increased, as in case (1), case (2) and case (3) or case (6), case (7) and case (8).

If the inlet mass fraction is increased, total heat transfer rate is increased as in case (6), case (7) and case (8). As case (1), case (4) and case (5) the higher domain width doesn't change total heat transfer rate. As the inlet temperature is increased, total heat transfer rate is changed so much case (1), case (2) and case (3). But the higher inlet velocity increases total heat transfer rate as in case (6), case (7) and case (8).

REFERENCES

Benelmir, R., Mokraoui, S., & Souayed, A. (2009). Numerical analysis of filmwise condensation in a plate fin-and-tube heat exchanger in presence of non-condensable gas, *International Journal Heat Mass Transfer, 45*, 1561–1573.

Cui, J., Li, W. Z., Liu, Y., & Zhao, Y.S. (2011). A new model for predicting performance of fin-and-tube heat exchanger under frost condition. *International Journal Heat and Fluid Flow*, 249–260.

Fossa, M., & Tanda, G. (2002). Free convection frost formation on a cold plate in a vertical channel. *1ˢᵗ International Conference of Heat Transfer, Fluid Dynamics and Thermodynamics (in South Africa).*

Hayashi, Y., Aoki, A., Adachi, S., & Hori, K. (1977). Study of frost properties correlating with frost formation types. *Journal of Heat Transfer*, *99*, 239–244.

Incropera, F. (2002). *Fundamentals of heat and mass transfer*. (5th ed.), John Wiley & Sons, Inc.

Jones, B.W., & Parker, J.D. (1975). Frost formation with varying environmental parameters, *Journal of Heat Transfer, 97*, 255–264.

Kakac, S. (1991). *Boilers, evaporators and condensers*. New York, USA: John Wiley.

Kakac, S., & Liu, H. (2002). *Heat exchangers-selection, rating and thermal design* (2nd ed.) Boca Raton, Florida, USA: CRC Press.

Kuan, D. Y., Aris, R., & Davis, H. T. (1984). Estimation of fin efficiencies of regular tubes arrayed in circumferential fins, *International Journal Heat Mass Transfer, 22*, 148-151.

Laaroussi, N., & Lauriat, G. (2008). Conjugate thermosolutal convection and condensation of humid air in cavities, *International Journal Thermal Sciences,47*,1571–1586.

Lenic, K., Trp, A., & Frankovic, B. (2009). Transient two-dimensional model of frost formation on a fin-and-tube heat exchanger, *International Journal Heat and Mass Transfer,22–32*

Liang, S.Y., Wong, T.N., & Nathan G.K. (2000). Comparison of one-dimensional and two-dimensional models for wet-surface fin efficiency of a plate-fin-tube heat exchanger, *Applied Thermal Engineering, 942–962*

Saboya, F.E.M., & Sparrow, E.M. (1974). Local and average transfer coefficients for one-row plate fin and tube heat exchanger configurations, *Journal Heat Transfer, 96,* 265–272.

Saboya, F.E.M., & Sparrow, E.M. (1976). Transfer characteristics of two-row plate fin and tube heat exchanger configurations, *International Journal Heat Mass Transfer,19*, 41–49.

Saboya, F.E.M., & Sparrow, E.M. (1976). Experiments on a three-row fin and tube heat exchanger, *Journal Heat Transfer, 98,* 520–522.

Sami, S.M., & Duong, T. (1989). Mass and heat transfer during frost growth, *Ashrae Transactions*, *95*, 158–223.

Seker, D., Karataş, H., & Egrican, N. (2004). Frost formation on fin-and-tube heat exchangers. Part I—Modeling of frost formation on fin-and-tube heat exchangers. *International Journal Refrigeration, 367–374.*

Shepherd, D.G. (1956). Performance of one-row tube coils with thin-plate fins, low velocity forced convection, *Heating, Piping Air Condition*, 28 , 137–144.

Sherif, S.A., Raju, S.P., Padki, M.M., & Chan, A.B. (1993). A semi-empirical transient method for modeling frost formation on a flat plate, *International Journal of Refrigeration*, *16*, 321–330.

Sparrow, E.M., Minkowycz, M.J., & Saddy, M. (1967). Forced convection condensation in the presence of noncondensables and interfacial resistance, *International Journal Heat Mass Transfer,10*,1829–1845

Yang, B., & Sekhar, S.C. (2007). Numerical algorithm studies of cfd modeling for a compartmented cooling coil under dehumidifying conditions, *Numerical Heat Transfer Part-A, 52*, 737–755.

Yonko, J.D., & Sepsy, C.F. (1967). An investigation of the thermal conductivity of frost while forming on a flat horizontal plate. *Ashrae Transactions,73*.

Tao, Y.X., Besant, R.W., & Mao, Y. (1993). Characteristics of frost growth on a flat plate during the early growth period, *Ashrae Transactions Symposium*, *93*, 746–799.

APPENDIX A

ANALYTICAL SOLUTION

Analytical solution of condensation on a flat plate is taken from Sparrow et al. (1967). Sparrow proves the impact of condensation. This proof is performed as forced condensation and calculations are computed analytically.

A.1 Liquid Boundary Layer

Liquid layer is very important for analysis. the conservation equations convert or constant fluid properties energy convection,

$$\frac{\partial u}{\partial x} + \frac{\partial v}{\partial y} = 0 \quad , \quad \frac{\partial^2 u}{\partial y^2} = 0 \quad , \quad \frac{\partial^2 T}{\partial y^2} = 0$$

$$(1)$$

Presenting transformed variables,

$$f''' = 0 \quad , \quad \theta'' = 0$$

where

$$\eta = y \sqrt{\left(\frac{U_\infty}{\vartheta_L x}\right)} \quad , \quad \psi = \left[\sqrt{(U_\infty \vartheta_L x)}\right] f(\eta) \quad , \quad \theta = \frac{T - T_w}{T_i - T_w}$$

where

u , v :   Velocity components

f :   Dimensionless stream function

θ :   Dimensionless temperature equation

η :   Similarity variable

U_∞ :   Free stream velocity

ϑ_L :   Condensed liquid kinematic viscosity

ψ :   Stream function

$$\frac{c_p(T_i - T_w)}{h_{f\theta}Pr} = \frac{1}{4}f_w''\eta_\delta^3 \tag{2}$$

Dimensionless society stays left side at the equation which repeats constantly in examination of condensation. Heat transfer rate is influenced from size of dimensionless society.

Where

c_p : Specific heat of condensate

h : Latent heat

Pr : Prandtl number of condensate

δ : Condensate layer thickness

w : At the wall

A.2 Velocity Problem in the Vapor-Gas Boundary Layer

Vapor-gas boundary layer includes four conservation laws: species conservation (one component), energy conservation, momentum conservation, and mass conservation for the mixture.

To advance, it is specially favorable to contend; momentum and continuity equations, and to temporarily delay the diffusion equation.

$$\frac{\partial u}{\partial x} + \frac{\partial v}{\partial y} = 0 \quad , \quad u\frac{\partial u}{\partial x} + v\frac{\partial u}{\partial y} = v\frac{\partial^2 u}{\partial y^2} \tag{3}$$

In this equation fixed properties are opined. The above equations are degraded to resemblance shape.

$$\xi = (y - \delta)\sqrt{\left(\frac{U_\infty}{\vartheta x}\right)} \quad , \quad \Psi = \left[\sqrt{(U_\infty \vartheta x)}\right]F(\xi) \tag{4}$$

From these,

$$F''' + \frac{1}{2}FF'' = 0 \tag{5}$$

where, the primes symbolize derivatives according to ξ. This can be specified that resemblance factor is described therefore $\xi = 0$ at interface. Also it occurs among vapor gas and liquid mixture.

Where

ξ : Similarity variable equation

Ψ : Stream function

(1) We assume the velocity u = 0 at the interface. Velocity of the interface has too low from U_∞, so that velocity can be ignored at the interface.

$$F'(0) = 0 \tag{6}$$

(2) There is mass at the interface. We have mass which is passing from gas side to liquid side. So, we have to consider convective and diffusive elements.

$$\dot{m} \, dx = \rho(u \, d\delta - v \, dx) - (j_v + j_g) \, dx \tag{7}$$

At the equation j_v is the vapor diffusive fluxes. Also j_g is the gas diffusive fluxes. But, $(j_v + j_g) = 0$. From these equations,

$$\dot{m} = \frac{1}{2} \left[\sqrt{\left(\frac{\rho \mu U_\infty}{x} \right)} \right] F(0) \tag{8}$$

From the upper equations, the $\dot{m}$ statements embodied, there follows,

$$F(0) = Rf(\eta_\delta)$$
(9)

where

$$R = [(\rho\mu)_L/(\rho\mu)]^{1/2}$$
(10)

(3) The shear stress $\tau = \mu(\partial u/\partial y)$ is permanent at the interface. We can write the shear continuity from converted factors.

$$F''(0) = Rf''(\eta_\delta)$$
(11)

(4) Velocity u approaches U_∞ and y approaches infinity. This situation takes the form,

$$F'(\infty) = 1$$
(12)

Additionally, from equations, it is clear that,

$$R\frac{c_p(T_i - T_w)}{h_{fg}Pr} = \left\{\frac{[F(0)]^3}{2F''(0)}\right\}^{1/2}$$
(13)

$$\eta_\delta = \left[\frac{2F(0)}{F''(0)}\right]^{1/2}$$
(14)

The $F(0)$ and $\varphi''(0)$ are displayed in the table 1 throughout with the suitable worths of $R[cp(T_i - T_w)/h_{fg}Pr]$ and η_δ^{-1} . Those last amounts are showed at figure A.1.
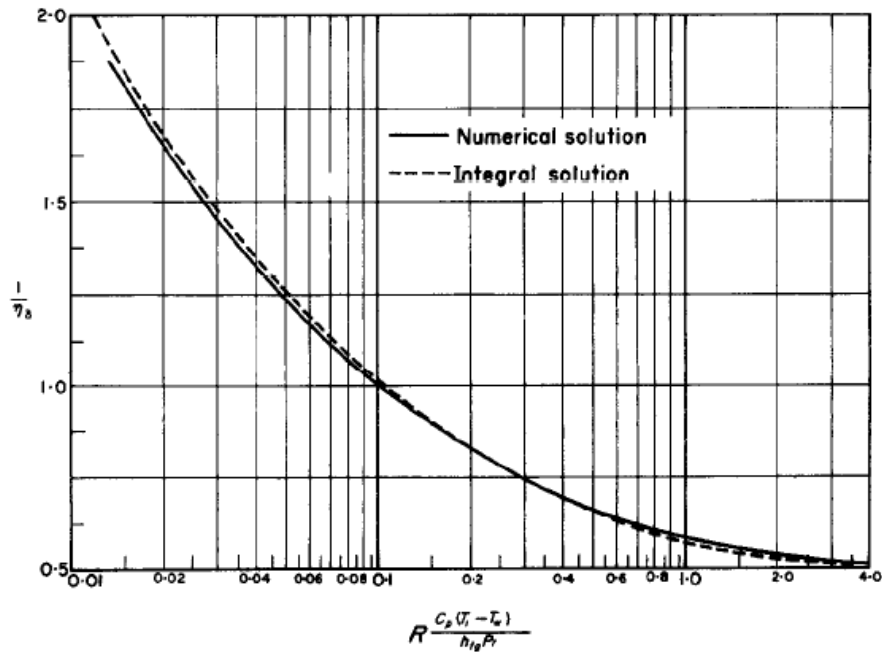
Figure A.1 Variation of l/η_δ, with R$c_p(T_i - T_w)$ / $h_{fg}Pr$. (Sparrow,1967)

Table A.1 Results Velocity and Diffusion Solution (Sparrow,1967)

$F(0)$	$F''(0)$	$R \dfrac{c_p(T_i - T_w)}{h_{fg} Pr}$	$\dfrac{1}{\eta_\delta}$	$\dfrac{W_\infty}{W_i}$
0·05	0·35026	0·013358	1·87150	0·95073
0·10	0·36867	0·036827	1·35770	0·90510
0·15	0·38730	0·066008	1·13620	0·86273
0·20	0·40612	0·099244	1·00760	0·82332
0·25	0·42514	0·13556	0·92210	0·78658
0·30	0·44434	0·17431	0·86053	0·75225
0·35	0·46371	0·21501	0·81391	0·72013
0·40	0·48325	0·25733	0·77721	0·69002
0·45	0·50296	0·30098	0·74755	0·66175
0·50	0·52282	0·34575	0·72306	0·63517
0·60	0·56300	0·43799	0·68494	0·58654
0·70	0·60373	0·53298	0·65668	0·54321
1·00	0·72887	0·82825	0·60368	0·43803
1·50	0·94542	1·3360	0·56138	0·31857
2·00	1·16943	1·8495	0·54069	0·24075
3·00	1·63223	2·8759	0·52157	0·14927
4·00	2·10740	3·8967	0·51325	0·10047
5·00	2·58990	4·9125	0·50890	0·07173
6·00	3·07708	5·9244	0·50638	0·05322
10·00	5·04852	9·9518	0·50242	0·02161

* For $Sc = 0.55$

44

A.3 The Diffusion Problem

Local mass fraction is displayed with 'W'. So,

$$W = \rho_g / (\rho_g + \rho_v) \tag{15}$$

Species conservation can be displayed for the noncondensable gas as below,

$$\rho u \frac{\partial W}{\partial x} + v \frac{\partial W}{\partial y} = D \frac{\partial^2 W}{\partial y^2} \tag{16}$$

from the equation diffusion coefficient is displayed with 'D'. Using similarity transformation, equations (4) and (5), and degraded mass fraction ϕ.

$$\phi = \frac{W - W_\infty}{W_i - W_\infty} \tag{17}$$

The diffusion equation can be expressed otherwise,

$$\phi'' + \frac{1}{2} Sc\, F\phi' \tag{18}$$

Interface mass fraction is showed with W_i in the equation and W_∞ is mass fractions of noncondensable gas at the inlet. Schmidt number is displayed with Sc. Also boundary conditions are showed below,

$$\phi(0) = 1 \quad , \quad \phi(\infty) = 0$$

From understanding equations, tightness situation occurs,

$$\rho_g \left(u \frac{d\delta}{dx} - \vartheta \right) = j_g = -\rho D \frac{\partial W}{\partial y} \tag{19}$$

Upper equality (19) is reformed to factors,

$$1 - \frac{W_\infty}{W_i} = -\frac{F(0) Sc}{2\phi'(0)} \tag{20}$$

Nevertheless, so single correlation is occurred among F(0) and $Rc_p(T_i - T_w)/h_{fg}Pr$, After that W_∞/W_i is regarded in form of equations.

Sc value is equalized 0,55. Therefore, W_∞/W_i is apprised to solve the heat transfer at the same Sc value. In the end calculations are displayed in Table A.1. Then chart is showed in Figure A.2.
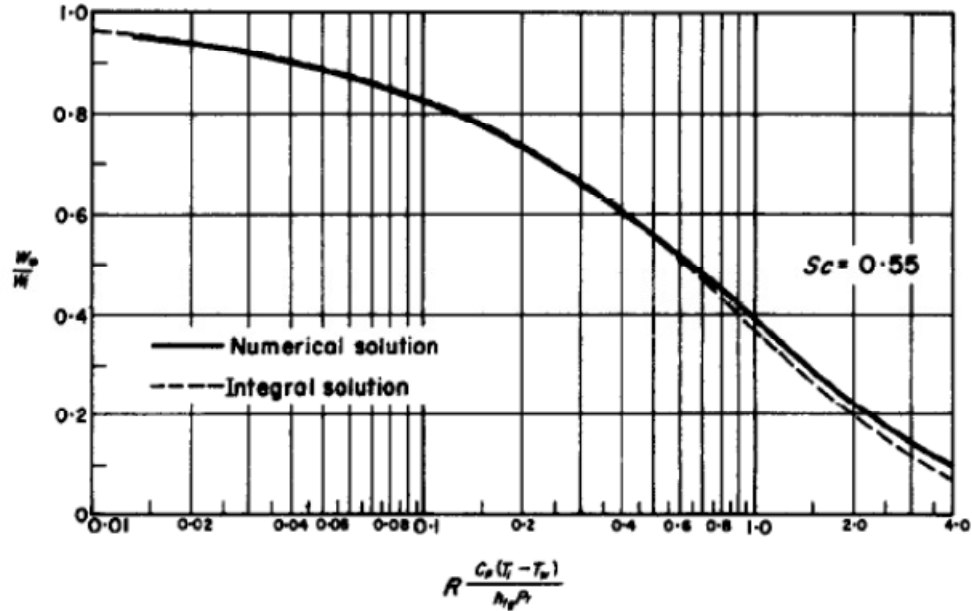

Figure A.2 Variation of W_∞/W_i with $Rc_p(T_i - T_w)/h_{fg}Pr$ for Sc=0.55 (Sparrow,1967)

A.4 Interface Temperature and Heat Transfer

If the condensation problem is examined, each rate of mixture elements are known to calculate the interface temperature: T_∞, W_∞, T_w. From knowledge, T_i temperature is defined to use in the equations.

p (total pressure) is considered in the first step. The perfect gases law is suitable for the total pressure to write equation like below,

$$\frac{p_v}{p} = \frac{1 - W}{1 - W\left(1 - M_v/M_g\right)}$$

(21)

Later, the heat transfer is calculated from T$_i$ value. So **q** displays the local heat transfer and the equation is below.

46

$$q = k_L \left(\frac{\partial T}{\partial y}\right)_{y=0} = \frac{k_L(T_i - T_w)}{\eta_\delta} \sqrt{\left(\frac{U_\infty}{\vartheta_L x}\right)} \qquad (22)$$

It is especially exciting to match the heat transfer rate. That condition of collation T_∞, T_w and U_∞, are taken same in two cases.

$$q_0 = \frac{k_{L,0}(T_\infty - T_w)}{\eta_{\delta,0}} \sqrt{\left(\frac{U_\infty}{\vartheta_{L,0} x}\right)} \qquad (23)$$

where $\eta_{\delta,0}$ is found from Fig. 1. by positing $(T_i - T_w)$ in the coordinate with $(T_\infty - T_w)$ and appraising the liquid features at T_∞. later, onto proportioning equations (22) and (23),

$$\frac{q}{q_0} = \left(\frac{1/\eta_\delta}{1/\eta_{\delta,0}}\right)\left(\frac{T_i - T_w}{T_\infty - T_w}\right)\left(\frac{k_L}{k_{L,0}}\right)\sqrt{\left(\frac{\vartheta_{L,0}}{\vartheta_L}\right)} \qquad (24)$$

where

W : Mass Fraction of gas

Sc : Schmidt Number

ρ : Density

Φ : Mass Fraction Variable

q : Heat Transfer Rate
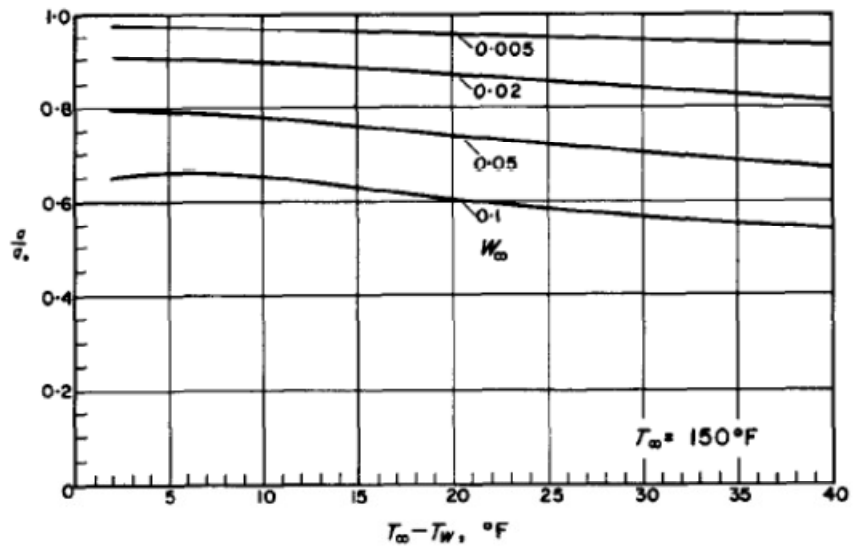
R : Property Ratio, $[(\rho\mu)_L/(\rho\mu)]^{1/2}$

Figure A.3 Heat transfer of condensation, $T_{\infty} = 65.5^{\text{o}}\text{C}$ (Sparrow,1967)

NOMENCLATURE

A	:	Area (m^2)
$A_{cellwall}$	:	First cell area above the wall (m^2)
c_p	:	Specific heat of condensate ($J\ kg^{-1}\ K^{-1}$)
$D_{i,m}$	:	Mass diffusion coefficient of species i in the mixture ($m^2\ s^{-1}$)
h	:	Enthalpy ($j\ kg^{-1}$)
J	:	Diffusion flux ($kg\ m^{-2}s^{-1}$)
k_L	:	Conductive heat transfer coefficient along the length ($W\ m^{-1}\ K^{-1}$)
L	:	Length of geometry (m)
$\dot{m}$	:	Mass flow ($kg\ s^{-1}$)
n	:	Normal vector
p	:	Pressure (Pa)
Pr	:	Prandtl number of condensate
q	:	Surface heat flux / Area ($W\ m^{-2}$)
R_i	:	Net rate of production of species i by chemical reaction
R	:	Property ratio, $[(\rho\mu)_L/(\rho\mu)]^{1/2}$
S	:	Width of geometry (m)
Sc	:	Schmidt number
S_{mass}	:	Mass source term ($kg\ m^{-3}\ s^{-1}$)
$S_{species}$	:	Species source term ($kg\ m^{-3}\ s^{-1}$)

S_{enerji}	:	Energy source term (J m^{-3} s^{-1})
T_{sat}	:	Saturation temperature (K)
u , v	:	x and y components of velocity (m s^{-1})
V_{cell}	:	First cell velocity (m s^{-1})
w	:	Mass fraction

Greek Symbols

θ	:	Dimensionless temperature equation
η	:	Similarity variable
ϑ_L	:	Condensed liquid kinematic viscosity (m^2 s^{-1})
ψ	:	Stream function
δ	:	Condensate layer thickness (m)
ξ	:	Similarity variable equation
Ψ	:	Stream function
ρ	:	Density (kg m^{-3})
Φ	:	Mass Fraction Variable

Subscripts

a	:	Dry air
Cell	:	First cell above the wall
H$_2$O	:	Water

i	:	Interface
m	:	Moist air
v	:	Water vapor
w	:	Wall
∞	:	Free stream condition